

8-2020

Modulating Avidity Of H8F4-Car By Regulation Of Expression Via Codon Modification

Rolando Vedia

Follow this and additional works at: https://digitalcommons.library.tmc.edu/utgsbs_dissertations

 Part of the [Immunotherapy Commons](#), and the [Laboratory and Basic Science Research Commons](#)

Recommended Citation

Vedia, Rolando, "Modulating Avidity Of H8F4-Car By Regulation Of Expression Via Codon Modification" (2020). *Dissertations and Theses (Open Access)*. 1027.

https://digitalcommons.library.tmc.edu/utgsbs_dissertations/1027

This Thesis (MS) is brought to you for free and open access by the MD Anderson UTHealth Houston Graduate School at DigitalCommons@TMC. It has been accepted for inclusion in Dissertations and Theses (Open Access) by an authorized administrator of DigitalCommons@TMC. For more information, please contact digcommons@library.tmc.edu.

**MODULATING AVIDITY OF H8F4-CAR BY REGULATION OF EXPRESSION
VIA CODON MODIFICATION**

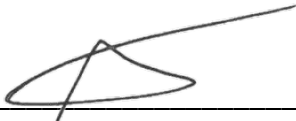
by

Rolando Antonio Vedia, B.S.

APPROVED:



Jeffrey Molldrem, M.D.
Advisory Professor



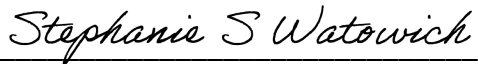
Gheath Al-Atrash, D.O., Ph.D.



Sijie Lu, Ph.D.



William Plunkett, Ph.D.



Stephanie Watowich, Ph.D.

APPROVED:

Dean, The University of Texas

MD Anderson Cancer Center UTHealth Graduate School of Biomedical Sciences

**Modulating Avidity of h8F4-CAR by Regulation of Expression
via Codon Modification**

A

THESIS

Presented to the Faculty of

The University of Texas

MD Anderson Cancer Center UTHealth

Graduate School of Biomedical Sciences

in Partial Fulfillment

of the Requirements

for the Degree of

MASTER OF SCIENCE

by

Rolando Antonio Vedia, B.S.

Houston, Texas

August 2020

Dedicated to Mom, Dad, Andy, Nana, Grandma, Grandpa Balde, and Grandpa Chema

Acknowledgements

I would like to thank my advisor and mentor Dr. Jeff Molldrem for taking me into his lab, allowing me to join the lab family, and supporting me in my training and goals. I would also like to thank Dr. Sijie Lu for co-mentoring and teaching me so many things and more and always being around to listen, help, guide, and support. Together, they've helped me start a path of study that I always dreamed of and now live every day. Words cannot express my thanks and gratitude.

Thank you to my advisory committee members Dr. Gheath Al-Atrash, Dr. Stephanie Watowich, and Dr. Bill Plunkett in addition to Dr. Molldrem and Dr. Lu. Your guidance has helped me gain confidence as a rising scientist and professional and inspire me to think in different, unique, and innovative ways.

Thank you to everyone from the TI/HBM lab family for always being there to answer my countless questions and help me troubleshoot everything that would go wrong and interpret everything that would go right. Thank you to the lunch group for making lunches the most interesting and hilarious times.

Thank you to the best friends I could have ever asked for and been blessed with -- Samantha, Amanda, Alyssa, Garcia, Cameron, and Johnny. Each of you are always there to pick me up when I'm down, listen whenever I need to talk, and make me laugh when I need it most. Thank you, thank you, thank you!

Thank you to my brother Andy. A constant source of laughter and someone who never ceases to make me smile even if I'm angry, sad, or, best, when I'm happy.

While this thesis is dedicated to them, I cannot help but thank them even more. Mom, Dad and Grandma as well as Nana, Grandpa Chema, and Grandpa Balde watching over me from

above. Your sacrifices, efforts, and love are without a doubt what have allowed me to make it this far and able to continue going. Thank you all for instilling in me the value of hard work, education, and, most of all, perseverance. Mom and Dad, words cannot express how much your words, advice, smiles, and love mean to me. Thank you all so much.

Modulating Avidity of h8F4-CAR by Regulation of Expression via Codon Modification

Rolando Antonio Vedia, B.S.

Advisory Professor: Jeffrey Molldrem, M.D.

Despite recent advances in the field of cancer immunotherapy and chimeric antigen receptor (CAR) therapies for the treatment of acute myeloid leukemia (AML), there is a need for more unique and innovative modalities to improve these therapies. Our group has extensively studied and demonstrated the potential of targeting the leukemia-associated antigen PR1 in the setting of AML. PR1 is an HLA-A2-restricted nonameric peptide derived from serine proteases neutrophil elastase and proteinase 3, is overexpressed on myeloid leukemia cells, and expressed at normal low levels in healthy hematopoietic cells. We have demonstrated efficacy in targeting PR1/HLA-A2 via the novel development of a TCR-like monoclonal antibody named 8F4 and its adaptation into a chimeric antigen receptor (CAR) named h8F4-CAR. As PR1/HLA-A2 is a self-antigen, its targeting renders increased susceptibility to on-target, off-tumor effects which is a common adverse effect seen in other CAR therapies targeting self-antigens. In an attempt to find an innovative manner to avoid this effect and optimize h8F4-CAR against the PR1/HLA-A2 complex, we investigated and conducted foundational studies using the genetic code and its inherent codon bias. This was done by altering serine and arginine residues within the non-variable regions of h8F4-CAR from their endogenous codons into the rare codon isoforms TCG and CGT for serine and arginine, respectively. Synonymous codon modification of h8F4-CAR represents a unique approach and strategy for modulating the affinity/avidity of CAR therapies by introducing rarer, or less frequently used, codons that encode the same residue. Data from

on-going studies in which rare synonymous codons were introduced show that expression of h8F4-CAR can be altered. While MFI values across different codon-modified construct iterations vary, immunoblotting results reveal presence of novel bands unique to codon-modified constructs compared to unmodified wildtype h8F4-CAR and control cells. The introduction of synonymous codon modifications, which takes advantage of inherent codon bias and frequency, represents a unique strategy to mitigate on-target, off-tumor effects. This strategy can be used to alter protein or biologic expression, providing a new approach to fine-tune and modulate CAR avidity and potency leading to greater efficacy by increasing therapeutic indices and reducing likelihood of adverse effects. These implications hold promise in not only in CARs but also in many adoptive cellular therapy platforms in which the genetic code can be utilized to improve and enhance therapies leading to favorable outcomes.

TABLE OF CONTENTS

| | |
|--|-------------|
| TITLE PAGE | II |
| DEDICATION | III |
| ACKNOWLEDGEMENTS | IV |
| ABSTRACT | VI |
| TABLE OF CONTENTS | VIII |
| LIST OF ILLUSTRATIONS/FIGURES | X |
| LIST OF TABLES | XII |
| CHAPTER 1: INTRODUCTION | 1 |
| ACUTE MYELOID LEUKEMIA | 1 |
| CANCER IMMUNOTHERAPY | 2 |
| LEUKEMIA-ASSOCIATED ANTIGEN PR1..... | 3 |
| CHIMERIC ANTIGEN RECEPTORS AND ASSOCIATED TOXICITIES..... | 5 |
| THE GENETIC CODE, CODON BIAS, AND CODON THERAPEUTICS..... | 10 |
| HYPOTHESIS & SPECIFIC AIMS | 14 |
| CHAPTER 2: H8F4-CAR CODON MODIFICATION | 16 |
| CODON MODIFICATION CONSTRUCT DEVELOPMENT..... | 16 |
| METHODOLOGY | 18 |
| CODON-MODIFIED H8F4-CAR CONSTRUCTION..... | 18 |
| PROKARYOTIC PLASMID SYNTHESIS..... | 20 |
| RETROVIRAL PACKAGING OF CODON-MODIFIED H8F4-CAR CONSTRUCTS..... | 22 |
| CHAPTER 3: CODON-MODIFIED H8F4-CAR TRANSDUCTION INTO JURKAT CELLS AS A MODEL SYSTEM.. | 25 |
| RETROVIRAL TRANSDUCTION OF H8F4-CAR CONSTRUCTS INTO JURKAT CELLS | 25 |

| | |
|--|-----------|
| METHODOLOGY | 26 |
| TRANSDUCTION PROCESS..... | 26 |
| FLOW CYTOMETRY PREPARATION AND STAINING | 27 |
| FLUORESCENCE-ACTIVATED CELL SORTING..... | 28 |
| DAY 7 ANALYSIS OF TRANSDUCED H8F4-CAR CELLS REVEALS SIMILAR CAR SURFACE EXPRESSION | 29 |
| FLOW CYTOMETRIC SURFACE EXPRESSION PATTERNS REMAIN CONSISTENT AND INDICATES | |
| EFFECTS OF RARE CODON MODIFICATION | 30 |
| CHAPTER 4: IMMUNOBLOTTING OF CODON-MODIFIED H8F4-CAR CONSTRUCTS | 35 |
| PROTEIN EXTRACTION FROM H8F4-CAR-TRANSDUCED CELLS..... | 35 |
| METHODOLOGY | 35 |
| CELL LYSIS AND PROTEIN EXTRACTION..... | 35 |
| GEL ELECTROPHORESIS AND IMMUNOBLOTTING..... | 36 |
| IMMUNOBLOTTING REVEALS ALTERED EXPRESSION OF CODON-MODIFIED H8F4-CAR | 39 |
| CHAPTER 5: DISCUSSION AND FUTURE DIRECTIONS..... | 49 |
| BIBLIOGRAPHY..... | 58 |
| VITA | 65 |

LIST OF ILLUSTRATIONS/FIGURES

| | |
|---|----|
| FIGURE 1: LINEAR CASSETTE VIEW OF WILDTYPE, UNMODIFIED H8F4-CAR | 7 |
| FIGURE 2: H8F4-CAR INTERACTION WITH PR1/HLA-A2-EXPRESSING AML BLAST | 7 |
| FIGURE 3: OVERVIEW AND RELATIVE LOCAITON OF CODON MODIFICATIONS IN SIX CODON- MODIFIED H8F4-CAR CONSTRUCTS | 18 |
| FIGURE 4: STEPWISE SCHEMATIC OF PROKARYOTIC PLASMID SYNTHESIS | 21 |
| FIGURE 5: STEPWISE SCHEMATIC PROCESS OF RETROVIRAL TRANSDUCTION AND CULTURING | 25 |
| FIGURE 6: H8F4-CAR SURFACE EXPRESSION AT DAY 7 POST-TRANSDUCTION USING PR1 TETRAMER AND ANTI-IGG (H+L) ANTIBODY THAT BANDS TO H8F4-CAR STEM..... | 30 |
| FIGURE 7: SORTING SCHEME FOR PR1/HLA-A2 TETRAMER SORTING OF CODON-MODIFIED CONSTRUCTS..... | 31 |
| FIGURE 8: PERCENTAGE POSITIVE BINDING AND MFI VALUES OF SORTED H8F4-CAR CONSTRUCTS AT TWO WEEKS POST-SORT | 32 |
| FIGURE 9: OVERVIEW OF RELATIVE PREDICTED ANTIBODY RECOGNITION REGIONS FOR PRIMARY IMMUNOBLOTTING ANTIBODIES USED..... | 37 |
| FIGURE 10: IMMUNOBLOTTING OF H8F4-CAR CONSTRUCTS AT DAY 7 POST-TRANSDUCTION | 40 |
| FIGURE 11: IMMUNOBLOTTING OF H8F4-CAR CONSTRUCTS AT TWO WEEKS POST-SORTING USING ANTI-HUMAN IGG ANTIBODY | 43 |
| FIGURE 12: CORROBORATORY IMMUNOBLOT EVIDENCE OF CODON MODIFICATION EFFECTS ALTERING H8F4-CAR EXPRESSION..... | 44 |
| FIGURE 13: CD3 ζ IMMUNOBLOTTING OF H8F4-CAR CONSTRUCTS AT TWO WEEKS POST-SORTING..... | 45 |

FIGURE 14: CD28 IMMUNOBLOTTING OF H8F4-CAR CONSTRUCTS AT TWO WEEKS POST-SORTING 47

FIGURE 15: FUTURE DIRECTIONS FOR H8F4-CAR CODON MODIFICATIONS..... 55

LIST OF TABLES

| | |
|--|----|
| TABLE 1: CODON USAGE FREQUENCY TABLE FOR THE HUMAN GENOME..... | 11 |
| TABLE 2: PHYSICAL VIRUS TITERS FOR H8F4-CAR UNMODIFIED AND CODON- MODIFIED PACKAGED RETROVIRUSES..... | 24 |

Chapter 1: Introduction

Acute Myeloid Leukemia

Acute myeloid leukemia (AML) is a malignant cancer of the blood which manifests as aberrant and unusual growth of healthy hematopoietic stem cells into leukemic progenitor cells and blasts. Often, these aberrant leukemic blasts accumulate a plethora of mutations which have been found to affect a variety of cell functions such as growth, differentiation, and proliferation. In addition, the proliferation of these blasts occurs at the expense of normal, healthy myeloid precursors and terminally differentiated cells like red blood cells, platelets, and granulocytes. Commonly characterized features of AML include fatigue, anemia, neutropenia, and thrombocytopenia, all of which are characteristic of bone marrow failure that occurs as AML progresses and leukemic blasts accumulate in the marrow (1,2). The National Cancer Institute's SEER (Surveillance, Epidemiology & End Results) Program estimates that 0.5% of men and women in the United States will develop AML over the course of their lives. The SEER program also estimates that AML diagnoses will account for 1.1% of new cancer diagnoses and 1.8% of all cancer deaths in the United States in 2020 alone. However, even more concerning is the 28.7% 5-year survival rate of the disease (3).

Treatment of AML typically consists of three phases: induction, consolidation and maintenance. Standard-of-care induction chemotherapy ranges from mid-to-high intensity for patients who can tolerate such doses, or lower-intensity for patients presenting with AML who cannot tolerate intense chemotherapy regimens. In addition, stem cell transplantation is another traditional therapeutic method for patients unable to achieve remission using conventional inductive/consolidative chemotherapy. Consolidation therapy typically consists of mid-to-lower

intensity chemotherapy. Beyond chemotherapy and stem cell transplantation, targeted therapies have recently risen to prominence in the treatment of AML as cytogenetic studies and understanding have improved (1,2). Recent studies from the Cancer Genome Atlas Research Network (NEJM, 2013) have identified nine functional categories of mutated genes in AML that have yielded an array of potential therapeutic options. Some of these functional categories include transcription factor fusions as well as mutations in tumor-suppressor genes and activated signaling genes (4). For example, aberrant signaling pathway activation is shown to stem from mutations in the tyrosine kinase receptor FLT3 which is commonly mutated in AML. This finding has given rise to the study and development of targeted FLT3 inhibitors as a targeted therapeutic strategy (5). In more recent years, incredible innovation and the emergence of cancer immunotherapy has undoubtedly bolstered study in additional potential therapeutic strategies to combat AML. This work will detail the development of a novel approach towards the modulation of an immunotherapeutic chimeric antigen receptor for the treatment of AML.

Cancer Immunotherapy

The immune system consists of a robust and intelligent machinery that is subdivided into two branches: adaptive and innate immunity. Adaptive immunity consists of B- and T-lymphocytes that engage and recognize a foreign antigen and begin mounting an immune response via clonal expansion over a period of time. Innate immunity consists of a variety of immune cells, such as natural killer (NK) cells and the various granulocytes, that provide rapid and continuous assault against foreign pathogens while working in tandem as adaptive immune response mounts. Together these two branches are critical towards the detection of cancer (6).

Furthermore, the understanding of these principles allows harnessing and development of potential immunotherapeutic strategies against cancer.

In the last couple of decades, cancer immunotherapy has certainly progressed to encompass a large variety of strategies (7). These strategies include the development of mono-specific antibodies, bi-specific antibodies, antibody-drug conjugates, chimeric antigen receptor T (CAR-T) cells, and immune checkpoint blockade therapies. A notable immunotherapy for the treatment of AML is the antibody gemtuzumab ozogamicin (anti-CD33) conjugated to the drug calicheamicin for the treatment of CD33-positive AML which has shown treatment improvements and increased survival (8). Additionally, the targeting of AML by CD123-specific chimeric antigen receptor therapy has been demonstrated by efficient targeting of CD123+ human AML blasts (9).

Leukemia-Associated Antigen PR1

The benefit of stem cell transplantation is seen in the ability to elicit graft-versus-leukemia (GvL) effects in patients. These benefits are demonstrated when cytotoxic T lymphocytes (CTL) from the donor are able to target and destroy leukemic blasts and their progenitors in the recipient. It is likely that this targeting is achieved via specific CTL interaction with a tumor-associated antigen (10,11). In the case of leukemia and AML, this occurs via recognition of a related antigen. These related antigens are classified into several categories including antigens expressed only in leukemia cells (leukemia-specific), those expressed mostly in leukemia cells and blasts but also in normal cells (leukemia-associated), antigens expressed in germline cells (cancer-testis antigens), and those ubiquitously expressed in the body (12). The targeting of these types of antigens in the setting of cancer immunotherapy has certainly grown and developed over the

years as our understanding has increased. Furthermore, criteria has been specified by the Translational Research Working Group of the National Cancer Institute to evaluate worthy antigens for study (13). This criteria has been further elucidated in the context of leukemia and AML. These criteria are: demonstrate leukemia specificity, antigen should be frequently found in leukemia cells and their progenitors, demonstrate an oncogenic role, demonstrate immunogenicity and ability to cause an immune response, and be clinically relevant (12).

The Molldrem group has focused its study on the leukemia-associated antigen, PR1. PR1 is a human leukocyte antigen (HLA)-A2*01-restricted nonameric peptide (VLQELNVTV) derived from serine proteases proteinase 3 (P3) and neutrophil elastase (NE) (14). Both P3 and NE are found as serine proteases within normal azurophilic granules as well as myeloid leukemia blasts. PR1 has been found to be overexpressed in leukemia blasts and its expression on blasts is recognized by PR1-specific CTL and results in preferential killing of blasts both in vitro and in vivo (15,16,17). Furthermore, targeting PR1 by vaccination has also been demonstrated in a Phase I/II clinical trial by our group and was found to induce antigen-specific immune response occurring early after vaccination as well as an increase in T cell receptor avidity of PR1-CTL (18).

In a novel therapeutic approach, a T cell receptor (TCR)-like monoclonal antibody named 8F4 (anti-PR1/HLA-A2) was developed against the PR1/HLA-A2 complex. 8F4 has demonstrated ability to lyse leukemic blasts and progenitors as well as inhibit leukemia progenitors but not normal, healthy progenitor growth in vitro (19). In vivo models have shown that 8F4 pre-treatment prevents AML engraftment, reduces established AML, prolongs survival, and reduces leukemia-initiating potential in mouse models (20).

With the success of 8F4, our group has developed additional therapies utilizing humanized 8F4 (h8F4) such as adaptation into a bi-specific T-cell engaging antibody (h8F4-BiTE) specific for CD3 which is ubiquitously expressed on T cells and for the PR1/HLA-A2 complex (21). Additionally, h8F4 has also been developed into a chimeric antigen receptor T cell (CAR-T) platform (22). As a chimeric antigen receptor therapy, h8F4-CAR shows promise as a very powerful therapeutic modality for AML. The development of these additional h8F4-bearing therapies seek to increase the potency of h8F4 against AML. While increasing potency of a therapy, the potential to increase cross-reactivity and on-target, off-tumor toxicity also occurs. This work demonstrates the foundational study to maintain specificity of h8F4-CAR against the PR1/HLA-A2 complex on AML cells while investigating a novel approach to modulate avidity to decrease potential for cross-reactive and on-target, off-tumor toxicity.

Chimeric Antigen Receptors and Associated Toxicities

Together with rise of immunotherapy as a whole, the study and implementation of chimeric antigen receptor T (CAR-T) cells as a therapeutic strategy has greatly increased. CAR-T cells are T lymphocytes genetically engineered to express a single chain fragment variable (scFv) from an antibody together with costimulatory and signaling moieties of the T cell receptor complex/co-complex. This engineering creates a chimeric receptor that harnesses the powerful specificity of B cell receptors or immunoglobulins with the cytotoxic and signaling capabilities of T cells. CAR-T cells have multiple generations that differ in the number of costimulatory or signaling domains they have. First generation CAR-T cells typically consist of the scFv, a hinge/transmembrane domain, and CD3 ζ domain of the TCR/CD3 complex. Second and third

CAR-T generations consist of the same domains but add one or two additional costimulatory domains, typically of the associated TCR complex such as CD28 or 4-1BB, respectively. The addition of more costimulatory and signaling domains to the CAR provides enhanced activation of the CAR-T cell (6,23,24).

CAR-T cells have primarily shown promising results in the treatment of blood cancers such as CD19 CAR for the treatment of B-cell acute lymphoblastic leukemia (B-ALL). Brentjens et al. (2013) demonstrated achievement of durable remissions as well as substantial expansion and persistence in B-ALL adult patients (25). Furthermore, recent approvals of Kite's Yescarta (axicabtagene ciloleucel) and Novartis' Kymriah (tisagenleucel) by the United States Food & Drug Administration (FDA) indicate efficacy and potential of CAR-T cell therapies (26). In the setting of acute myeloid leukemia, CAR-T cell therapy potential is also under investigation. CD33 CAR-T cells have shown in vitro activity against AML cell lines and primary samples as well as reduction in leukemia burden and survival advantages in vivo (27). As previously described (22), and shown below in Figures #1 and 2, to increase the efficacy of the h8F4 antibody, our group has developed a 2nd-generation chimeric antigen receptor, h8F4-CAR. H8F4-CAR consists of the h8F4 scFv (VH and VL2 regions), a G₄S linker, an IgG1 CH₂CH₃ extracellular hinge/stem, a CD28 transmembrane and intracellular costimulatory domain, and a CD3 ζ intracellular signaling domain.

Figure #1. Linear cassette view of wildtype, unmodified h8F4-CAR.

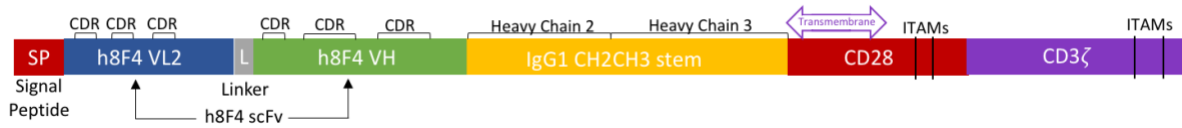


Figure #1. Linear cassette view of wildtype h8F4-CAR. Sequence begins with a signal peptide and includes variable light chain 2 and variable heavy chain of the h8F4-CAR scFv linked together with a G₄S linker. Extracellular hinge/stem region of h8F4-CAR consists of IgG1 constant heavy chains 2 and 3. Transmembrane and a portion of the intracellular region consists of CD28 as well as an fully intracellular CD3 ζ region. Relative positioning for CDR (complementarity-determining regions), IgG1 CH2 and CH3 regions, transmembrane (TM), and ITAMs (immunoreceptor tyrosine-based activation motif) locations are specified.

Figure #2. H8F4-CAR interaction with PR1/HLA-A2-expressing AML blast.

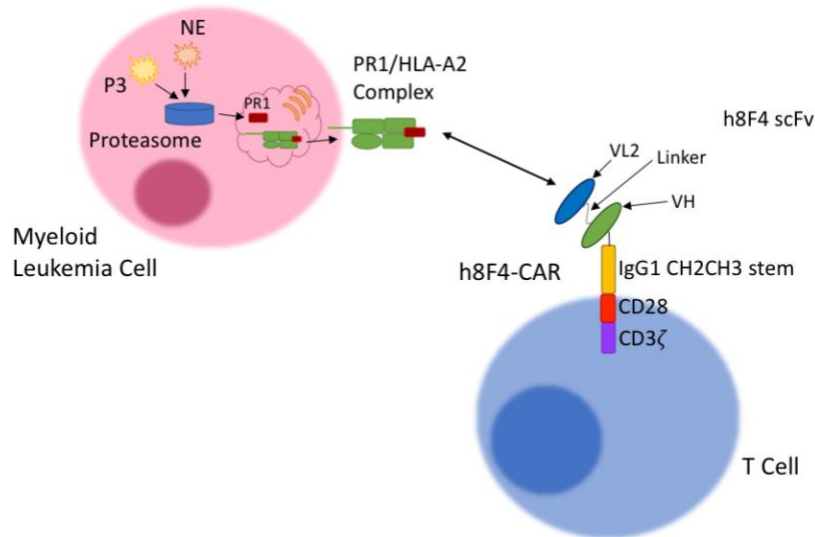


Figure #2. General schematic of PR1/HLA-A2-presentation on AML cell surface and interaction with h8F4-CAR. H8F4-CAR components and relative positioning shown above. H8F4-CAR

recognizes surface-presented PR1/HLA-A2 on the AML cell surface and can elicit cytotoxic effects and immune response.

h8F4-CAR maintains recognition of PR1/HLA-A2 and specifically mediates anti-leukemic activity against PR1/HLA-A2-expressing AML cell lines and primary AML blasts in vitro (22). The benefit of targeting PR1/HLA-A2 using h8F4-CAR has also been demonstrated by our group in PDX models where h8F4-CAR can effectively target AML within the central nervous system unlike naked h8F4. Ultimately, this demonstrates the powerful potential of h8F4-CAR as a CAR-T cell therapy for the treatment of acute myeloid leukemia.

Unfortunately, CAR-T cell therapies are not without associated toxicities that range in severity and reversibility that occur in a variety of mechanisms. One of the most common toxicities seen as a result of CAR-T cell therapy is cytokine release syndrome (CRS). CRS is caused by large-scale immune activation and release of cytokines as a result of CAR-T therapy. Further, CRS can result in clinical features like fatigue, nausea, tachycardia, liver failure, hypotension, myalgia, renal impairment, and overall life-threatening clinical presentations. In addition to possibility of CRS, CAR-T cell therapy-associated toxicities include neurological toxicity, anaphylaxis, graft vs. host disease (GvHD), and on-target, off-tumor reactivity (23, 28). Furthermore, common issues in the field of CAR-T therapies include CAR-T cell exhaustion and persistence which require innovative strategies to improve (29). In the case of h8F4-CAR, its target PR1/HLA-A2 is also normally expressed at low-levels on healthy hematopoietic cells but overexpressed on myeloid leukemia cells. This suggests potential for on-target, off-tumor toxicity. On-target, off-tumor effects have also been seen in CD19 CAR to treat B-ALL since CD19

is endogenously expressed on B-cells. On-target, off-tumor toxicity as a result of CD19 CAR has been shown to result in B-cell aplasia, which is the elimination of both normal and malignant B cells (24).

Fortunately, there is an assortment of treatments to combat CAR-T cell-related toxicities. However, many of these therapies are reactive and not proactive. Recent research has shown promising results in proactive methods to prevent CAR-T cell toxicity such as introduction of a “suicide” gene to eliminate CAR-T cells within the body should related toxicities become unmanageable (30). Additionally, methods to introduce temporary, transient CAR-T cell therapy is also under investigation (31). Because of the known issues surrounding CAR-T cell therapy toxicity, it is the goal of this work to introduce and detail the initial and on-going development of a proactive method to prevent or modulate CAR-T therapy in the setting of h8F4-CAR using the natural genetic code and codon bias. H8F4-CAR represents a prime candidate to study novel and unique methodologies such this to address cross-reactivity and on-target, off-tumor effects as a result of potent CAR therapies. As a first-in-class, TCR-like monoclonal antibody adapted in a CAR, h8F4-CAR is ideal due to its high avidity and potency against the PR1/HLA-A2 complex, which is a self-antigen. Furthermore, identifying a unique method to improve and enhance h8F4-CAR using the natural genetic code and codon bias by modulating avidity can hold promise when used in other CAR platforms or adoptive cellular therapy platforms.

The Genetic Code, Codon Bias, and Codon Therapeutics

The genetic code consists of the 64 codons that encode for the 20 standard amino acids. These amino acids serve as the fundamental building blocks of all proteins within our body and those of most living organisms on Earth. Our genetic code is degenerate and redundant in that the 20 standard amino acids have between one and six codons that can encode for them at varying frequencies. The amino acid serine, for example, has six codons that can encode for it. These six codons are used at varying frequencies within the human genome. This means that of these six codons, there is one codon that is used more often than the others and another codon that is used the least of all the other codons. This principle is the basis of codon bias. Codon bias is maintained across codons and has been used as the basis for developing methods to alter rates of expression to improve therapies. Table #1 provides codon fractions where bias between codons for amino acids are clearly demonstrated.

Table #1. Codon usage frequency table for the human genome.

| Codon | Amino Acid | Fraction | Codon | Amino Acid | Fraction |
|------------|------------|-------------|------------|------------|-------------|
| TTT | F | 0.45 | TCT | S | 0.18 |
| TTC | F | 0.55 | TCC | S | 0.22 |
| TTA | L | 0.07 | TCA | S | 0.15 |
| TTG | L | 0.13 | TCG | S | 0.06 |
| TAT | Y | 0.43 | TGT | C | 0.45 |
| TAC | Y | 0.57 | TGC | C | 0.55 |
| TAA | Stop | 0.28 | TGA | Stop | 0.52 |
| TAG | Stop | 0.20 | TGG | W | 1.00 |
| CTT | L | 0.13 | CCT | P | 0.28 |
| CTC | L | 0.20 | CCC | P | 0.33 |
| CTA | L | 0.07 | CCA | P | 0.27 |
| CTG | L | 0.41 | CCG | P | 0.11 |
| CAT | H | 0.41 | CGT | R | 0.08 |
| CAC | H | 0.59 | CGC | R | 0.19 |
| CAA | Q | 0.25 | CGA | R | 0.11 |
| CAG | Q | 0.75 | CGG | R | 0.21 |
| ATT | I | 0.36 | ACT | T | 0.24 |
| ATC | I | 0.48 | ACC | T | 0.36 |
| ATA | I | 0.16 | ACA | T | 0.28 |
| ATG | M/Start | 1.00 | ACG | T | 0.12 |
| AAT | N | 0.46 | AGT | S | 0.15 |
| AAC | N | 0.54 | AGC | S | 0.24 |
| AAA | K | 0.42 | AGA | R | 0.20 |
| AAG | K | 0.58 | AGG | R | 0.20 |
| GTT | V | 0.18 | GCT | A | 0.26 |
| GTC | V | 0.24 | GCC | A | 0.40 |
| GTA | V | 0.11 | GCA | A | 0.23 |
| GTG | V | 0.47 | GCG | A | 0.11 |
| GAT | D | 0.46 | GGT | G | 0.16 |
| GAC | D | 0.54 | GGC | G | 0.34 |
| GAA | E | 0.42 | GGA | G | 0.25 |
| GAG | E | 0.58 | GGG | G | 0.25 |

Table #1. Emboldened and highlighted codons within the table are examples of rare codons present within the codon populations. These are targeted as rare codons to test and study their effects and efficiency in sequences and through transcription and translation. Codons such

as the TCG and CGT codons for serine and arginine, respectively, are more rare in fraction than other rare codons. Fractions represent usage compared to codons within the pool that encode for the same amino acid. Further, this translates to lower presence in frequency per thousand codons (data not shown). Table was adapted and values taken from the GenScript Codon Usage Frequency Tool.

Existing methodologies utilizing codon bias in therapeutics include codon optimization and codon modification. Codon optimization involves altering all codons within a sequence, such as the sequence of a biologic agent or protein, to improve and theoretically maximize biologic/protein expression. Codon optimization has previously been investigated, such as in gene therapy research for treatment of hemophilia A by targeting human factor VIII. This investigation studies the utilization of codon bias to modify codons synonymously into their more commonly used counterparts based on codon usage tables in order to increase or maximize protein expression. Deficiency or low expression of human factor VIII is caused by inefficient factor VIII mRNA expression as well as protein misfolding. Ward et al. (2011) demonstrated that codon optimization of factor VIII cDNA constructs achieved 29- to 44-fold increase in expression which shows desirable results to combat human factor VIII deficiency and hemophilia A. These results demonstrate codon optimization therapy potential (32). The promising effects of codon optimization has also been demonstrated in adoptive cell therapies such as adoptive T cell receptor therapy. Scholten et al. (2006) demonstrated marked improvement in functional expression of transgenic human T cell receptors when the TCR α and β chains were codon-

optimized compared to wildtype counterparts (33). Advantages of codon optimization have also been noted in chimeric antigen receptor T cell therapy (34).

Codon optimization is an attractive option to improve biologic therapies. However, in certain settings, codon optimization may not be the best route to pursue. H8F4-CAR, for example, may not be the best candidate for codon optimization. As previously mentioned, h8F4-CAR targets PR1/HLA-A2, a self-antigen overexpressed on myeloid leukemia cells and normally expressed at low-levels in hematopoietic cells. Codon optimization to maximize h8F4-CAR expression and efficacy has potential to introduce additional risk of on-target, off-tumor toxicity to healthy cells. Fortunately, there are other codon therapy strategies. Codon modification utilizing codon bias provides a unique and novel method to improve both h8F4-CAR and adoptive cell therapies as a whole. Hoekema et al. (1987) demonstrated in the PGK1 gene of *Saccharomyces cerevisiae* that substitution of codons into their rare, or least frequently abundant, isoform in increasing numbers led to decreased expression of the PGK1 protein. It was posited that increasing substitutions into rare codons led to impaired elongation due to low tRNA pools for their cognate rare codon leading to mRNA destabilization and ribosomal pausing. As a result, PGK1 expression was diminished (35). Utilizing the concept of codon substitution and modification, this can be applied to find novel and unique methods to improve adoptive cellular therapy strategies such as CAR-T therapies. Based on this concept and supportive findings, we decided to apply codon modification and substitution to investigate potential to modulate the expression and functional avidity of h8F4-CAR for optimal avidity to the PR1/HLA-A2 complex.

Hypothesis and Specific Aims

We hypothesize that synonymous codon modification of h8F4-CAR to demonstrate reduced expression against PR1/HLA-A2 may provide a method to allow modulation of functional avidity of h8F4-CAR. Because PR1/HLA-A2 is a self-antigen expressed on normal hematopoietic cells but overexpressed on AML cells, the high avidity of h8F4-CAR and its potency has the potential to cause varying levels of on-target, off-tumor toxicity reducing its therapeutic index. Synonymous codon modification of h8F4-CAR represents a unique approach and strategy for modulating the affinity/avidity of CAR therapies by introducing rare synonymous codon changes to attain an optimal avidity that effectively targets overexpressed antigen on cancer cells and spares cytotoxic effects on normal cells. In addition, codon modification may also provide a method to increase persistence and reduce non-specificity of CAR-T therapies. To investigate the potential and resulting effect of codon modification in h8F4-CAR, the following aims will be employed:

AIM 1: To develop and construct h8F4-CAR iterations with rare codon modification of amino acid residues to study whether modification of residues in the IgG1 CH2CH3 domain, CD28 costimulatory domain, and CD3 ζ signaling domain of h8F4-CAR will alter h8F4-CAR expression.

AIM 2: To test and determine whether introduced rare codon modification of amino acid residues within h8F4-CAR will alter h8F4-CAR expression, allow modulation of avidity, and maintain specificity for the PR1/HLA-A2 complex.

Our goal is to develop a novel and unique strategy utilizing codon bias and codon modification as a therapeutic method to improve chimeric antigen receptor T-cell therapies and adoptive cellular therapies as a whole. This project has the potential to bring forward new strategies to the design, development, and optimization of CAR therapies not only for the treatment of AML but other malignancies as well. Modulation of CAR therapies by regulating and tuning expression and avidity can further improve patient treatment by increasing therapeutic indices and reducing likelihood of unwanted cytotoxicity.

Chapter 2: h8F4-CAR Codon Modification

Codon Modification Construct Development

Wildtype, unmodified h8F4-CAR, as described by Ma et al. (2016) and as shown in Figure #1 was extensively studied at the codon-level to determine possible iterations of h8F4-CAR that could be developed to study the effects of codon-modification in h8F4-CAR. In order to maintain h8F4-CAR specificity towards the PR1/HLA-A2 complex in the first phase of codon modification testing, it was decided to limit codon modifications and substitutions to only the IgG1 CH2CH3 hinge/stem extracellular region, the CD28 transmembrane and intracellular costimulatory region, and the CD3 ζ intracellular signaling region. Therefore, the initial signal peptide, h8F4 scFv, and its G₄S linker sequence did not feature any codon modifications or substitutions at all.

The three regions that would feature codon modification were analyzed at the codon-level using codon frequency tables for the human genome to quantify the number of codon isoforms present for amino acids determined to be best for rare codon substitution and modification. These amino acids were also determined using a codon frequency usage table. Table #1 demonstrates the variety in codon usage using a codon frequency table for the human genome. Using the table, we looked at all 20 standard amino acids that had between two and six codons that encoded for its cognate amino acid at less than 8% overall frequency per thousand codons within the human genome compared to its other respective isoforms. This yielded a variety of potential amino acids and their rare codons that could be used to modify h8F4-CAR. These included the TCG codon for serine, the GTA codon for valine, the CTA or TTA codons for leucine, the ATA codon for isoleucine, the CGT codon for arginine, and the ACG codon for threonine as well as a few others. Once these rare codons for these amino acids were

determined, they were then studied, analyzed, and quantified across the three regions for location, density, and distribution. Of these, the rare TCG codon for serine showed good distribution within the three regions and was not endogenously present within the regions. In addition, the rare CGT codon for arginine also showed good distribution with the three regions and was sparingly endogenously present within the regions. The rare TCG and CGT codons for serine and arginine, respectively, were selected for rare codon modification within the IgG1 CH2CH3 extracellular hinge, the CD28 transmembrane and intracellular costimulatory region, and the CD3 ζ intracellular signaling region of h8F4-CAR.

After determining which codons would be modified within the h8F4-CAR sequence into rare codons, several iterations and constructs were created to test the effect of codon modification in h8F4-CAR in terms of location and density. Six constructs were developed. These constructs varied by which amino acid was codon-modified (serine, arginine, or a combination of both), location (both extracellular and intracellular or intracellular only), and density (denser extracellularly or intracellularly). These constructs were named S30, S7(i), S6(i), R27, R21(i), and RS30(i). Figure #3 provides a general breakdown of the six constructs as well as relative position of rare codon modifications for visualization. Nomenclature for these fragments/constructs was the following: amino acid residue altered, number of codons changed, and whether codon modification was intracellular-restricted. For example, the RS30(i) construct features both arginine and serine residues that were codon-modified, 30 total codon modifications, and all codons modified were completely located within the intracellular regions (i).

Figure #3. Overview and relative location of codon modifications in six codon-modified h8F4-CAR constructs.

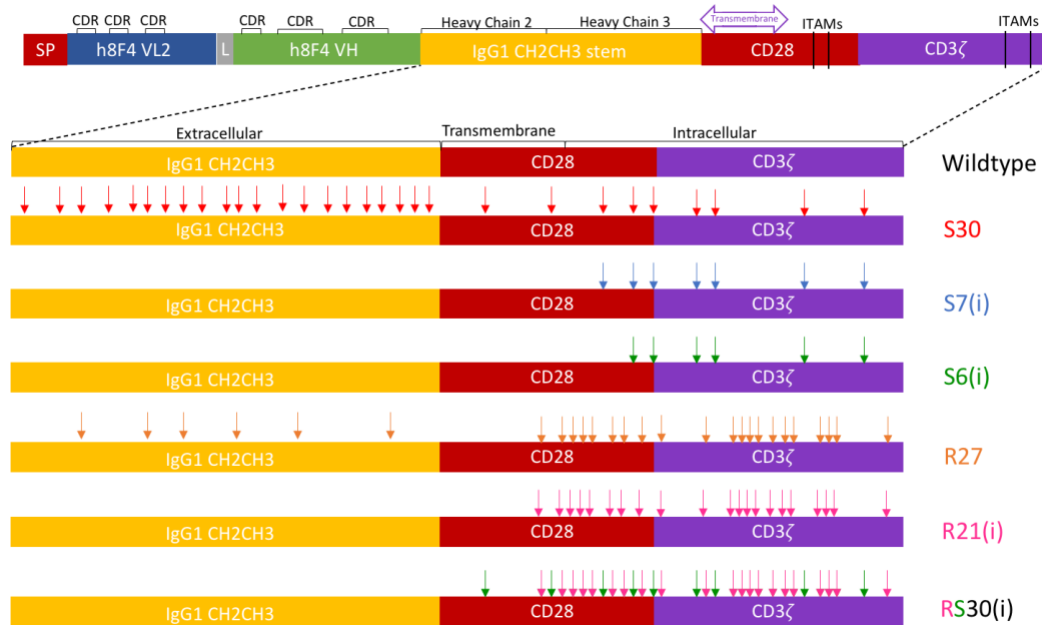


Figure #3. General scheme and overview of the six codon-modified h8F4-CAR constructs compared to wildtype, unmodified h8F4-CAR. Relative location and positions of codons that were modified into respective rare codons are provided for enhanced visualization.

Methodology

Codon-Modified h8F4-CAR Construction

A “cut-and-paste” method to introduce insert sequences featuring rare codon modification in the designated regions (IgG1 CH2CH3 stem, CD28, and CD3ζ) was used by taking wildtype, unmodified h8F4-CAR, removing endogenous regions, and replacing with rare codon-modified insert sequences. The removal of endogenous regions was facilitated by restriction enzyme digestion. Constructs that featured codon modification across all three regions (S30 and

R27) were developed using the endogenous BamHI and SphI enzyme digestion sites within h8F4-CAR. Constructs that featured codon modification only intracellularly (S7(i), S6(i), R21(i), and RS30(i)) were constructed using the endogenous NsiI and SphI enzyme digestion sites within h8F4-CAR.

The sequences for each codon-modified construct were created *in silico* by modifying the endogenous serine or arginine codons into their selected rare codon isoform with the online SnapGene software using template wildtype, unmodified h8F4-CAR sequence. Following *in silico* construction, double-stranded sequences were synthesized by Integrated DNA Technologies.

For construction of h8F4-CAR codon-modified constructs, insert gene fragments received for each construct and wildtype, unmodified h8F4-CAR plasmid was subjected to restriction enzyme digestion. Wildtype, unmodified h8F4-CAR plasmid was used as vector for plasmid synthesis by using restriction enzyme sites BamHI and SphI or NsiI and SphI for removal of endogenous sequence to allow for insertion of codon-modified sequences. Restriction enzyme digestion using BamHI and SphI sites was done for wildtype, unmodified h8F4-CAR plasmid as well as received S30 and R27 gene fragments. In parallel, digestion using NsiI and SphI sites was done for wildtype, unmodified h8F4-CAR plasmid as well as received S7(i), S6(i), R21(i), and RS30(i) gene fragments. Following vector enzyme digestions, vectors were dephosphorylated to enhance and increase ligation efficiency to inserts which were not dephosphorylated. All restriction enzymes and phosphatase were purchased from New England Biolabs. Following insert and vector digestions and dephosphorylation, samples were run on an agarose gel and appropriate bands for digested vectors and inserts were excised and extracted. Gel extractions were completed as instructed using a QIAGEN Gel Extraction Kit (#28706) and quantified.

Following quantification, vectors and inserts were ligated together. BamHI and SphI-digested wildtype, unmodified vector was ligated to digested S30 and R27 inserts independently. Likewise, NsiI and SphI-digested wildtype, unmodified vector was ligated to digested S7(i), S6(i), R21(i), and RS30(i) inserts independently. This essentially allowed a “cut-and-paste” method of replacement for endogenous IgG1 CH2CH3 hinge, CD28, and CD3 ζ regions with codon-modified IgG1 CH2CH3 hinge, CD28, and CD3 ζ regions. Ligation mixtures were mixed and allowed to ligate overnight for prolonged ligation reaction time.

Prokaryotic Plasmid Synthesis

Following ligation, constructs were transformed into Stbl3 chemically competent *Escherichia coli* cells (Invitrogen) as instructed (#C7373-03). Cells were streaked onto agar plates treated with carbenicillin for selection of successful transformants. Up to 10 colonies were picked per transformation and placed into bacterial culture tubes with carbenicillin-treated LB broth and grown overnight. After overnight culturing, a portion of each culture was prepared and plasmid purified using the QIAGEN QIAPrep Spin Miniprep Kit according to manufacturer’s instructions (QIAGEN #27106). Diagnostic enzyme digestion was done on samples to assess whether there was successful insertion of product based on molecular weight. Samples/plasmids determined to be successfully transformed were then sent to the MD Anderson Advanced Technology Genomics Core Facility for sequencing using the following primers.

- h8F4-CAR Vector 5’ primer: 5’ AGACGGCATCGCAGC
- h8F4-CAR Upstream CH2 primer: 5’ TTTACTGGGGCCAAGG
- h8F4-CAR CH2 primer: 5’ GAGCCCAAATCTCTCTG

- h8F4-CAR SFG 3' primer: 3' AACTAGAGCCTGGACC

Once sequences were returned, sequences were analyzed and aligned with their respective templates using the online SnapGene software. Additionally, they were cross-checked using the sequences returned from all primers for a given prep to produce a continuous sequence and verification of a flawless sequence.

Figure #4. Stepwise schematic of prokaryotic plasmid synthesis.

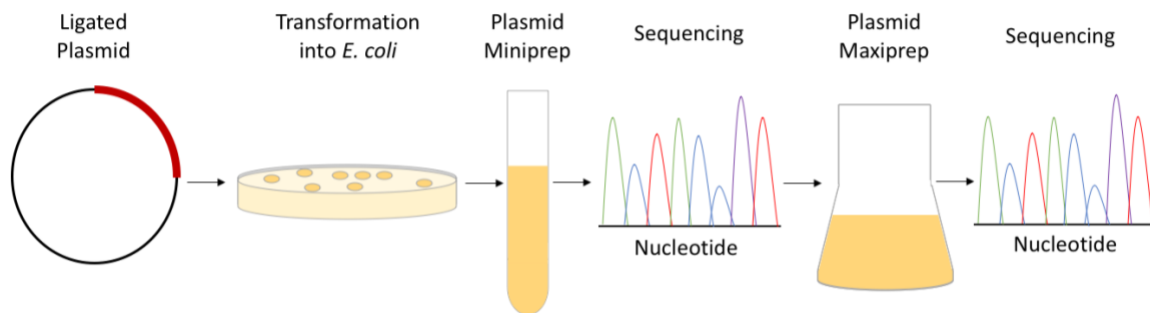


Figure #4. Stepwise schematic of prokaryotic plasmid synthesis. Following successful ligation of codon-modified h8F4-CAR plasmids, plasmids were transformed and grown in chemically competent *E. coli* cells. Between plasmid mini- and maxi-preps and in conjunction with sequencing, plasmid preps were also subjected to diagnostic restriction enzyme digestion.

Following identification and verification of flawless sequences for a plasmid prep, the remaining stored bacterial culture was grown at a large-scale for greater isolation and purification of plasmid. These cultures were then used to prepare and purify plasmid maxiprep to be able to begin producing virus. Plasmid maxiprep was prepared using the Plasmid Plus Maxiprep Kit as instructed by manufacturer (QIAGEN #12963), quantified, and brought to a

standard concentration and stored until further use. Following production and purification of larger-scale plasmid quantities, codon-modified h8F4-CAR constructs were prepared for retroviral packaging for transduction into cells. Stepwise schematic for prokaryotic plasmid synthesis is shown in Figure #4.

Retroviral Packaging of Codon-Modified Constructs

Using plasmid maxipreps with confirmed flawless sequences for each h8F4-CAR codon-modified construct, each construct was packaged into a retroviral system for viral transduction into cells. 293GP cells were used for retroviral packaging. Cells were seeded onto plates and transfected by way of lipofection. Lipofection consisted of two separate reactions. One reaction contained Lipofectamine 2000 reagent (Invitrogen #11668-019) and Opti-MEM medium (Gibco #31985-062). The second reaction contained plasmid of interest for transfection (each h8F4-CAR construct), viral helper plasmid (RD-114 envelope), and Opti-MEM medium. Both reactions were mixed together and incubated briefly before conducting lipofection and incubating for a 6 hour period. Following lipofection, viruses were harvested three times by collecting culture supernatant and replacing with fresh 293GP culture medium. 293GP culture medium consisted of DMEM High Glucose medium (GE HyClone #SH30022.01) supplemented to 10% with heat-inactivated fetal bovine serum (Corning #35-010-CV) and to 1% with penicillin/streptomycin solution (GE HyClone #SV30010). Harvested viral supernatant was removed of packaging cells and debris and supernatants were stored until further use.

Once retroviral supernatants were collected, supernatants were then titrated to determine physical viral titers (virus particles per milliliter – VP/mL) prior to transducing into a

cell line. Retroviral supernatant collections were titrated using the Cell Biolabs QuickTiter Retrovirus Quantitation Kit as instructed (Cell Biolabs #VPK-120) and quantified. Table #2 shows the results of physical virus titration in virus particles per milliliter (VP/mL). Infectious titer is predicted to be 100 to 1000 of physical viral titer. Because physical virus titers were similar in order of magnitude, this suggested that when transduced into cells, similar transduction efficiency was anticipated across the cultures.

Table #2. Physical virus titers for h8F4-CAR unmodified and codon-modified packaged retroviruses.

| PHYSICAL VIRUS TITER (VP/mL) - virus particles/mL | |
|--|----------------------------|
| <i>Construct</i> | <i>Virus titer (VP/mL)</i> |
| h8F4-CAR Wildtype | 8.869×10^{14} |
| S30 | 3.942×10^{13} |
| S7(i) | 4.426×10^{13} |
| S6(i) | 6.029×10^{13} |
| R27 | 5.934×10^{13} |
| R21(i) | 6.671×10^{13} |
| RS30(i) | 4.159×10^{13} |

Table #2. Summarization of physical virus titers for h8F4-CAR constructs. Physical virus titers were quantitated using retroviral RNA from each retrovirus isolated and purified from the Cell Biolabs QuickTiter Retrovirus Quantitation Kit (Cat# VPK-120).

Chapter 3: Codon-Modified h8F4-CAR Transduction into Jurkat Cells as A Model System

Retroviral Transduction of h8F4-CAR constructs into Jurkat Cells

Following retroviral packaging and titration, retroviruses harboring h8F4-CAR codon-modified constructs were then prepared for transduction into a mutant Jurkat cell line (J.RT3-T3.5) deficient of T cell receptor (TCR) β chain, hereby referred to as Jurkat $-\beta$. TCR β chain deficiency renders the cells to lack endogenous TCR complex. Because CAR-T cells are TCR-independent, this cell line served as a beneficial model cell line to begin testing codon-modified h8F4-CAR constructs. The retroviral transduction process is schematically shown in Figure #5.

Figure #5. Stepwise schematic process of retroviral transduction and culturing.

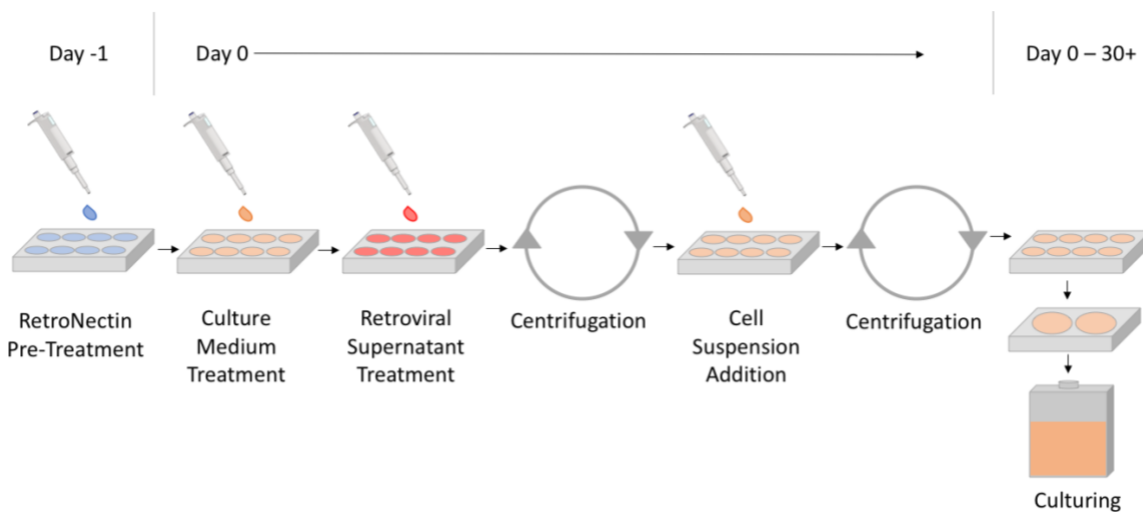


Figure #5. Stepwise process of retroviral transduction of h8F4-CAR codon-modified constructs into Jurkat $-\beta$ cells is schematically demonstrated above. Prior to treatments and addition during day zero steps, RetroNectin pre-treatment, culture medium treatment, and retroviral

supernatant treatments were all aspirated before addition of next treatment. Plates and flask are not drawn to scale and are meant for visualization purposes.

Methodology

Transduction Process

Retroviral transduction consisted of multi-day preparation and following day 0 of transduction, required careful culturing as well as a time course study. Since the Jurkat - β cell line does not require activation nor stimulation, pre-transduction preparation consisted of coating RetroNectin reagent (Takara #T100A) in a non-tissue culture plate with sterile PBS (Lonza #17-516F). RetroNectin coating allows for co-localization of cells and virus during the transduction process to improve transduction efficiency. Since wildtype, unmodified h8F4-CAR and the 6 codon-modified h8F4-CAR constructs were transduced, 7 wells were prepared and coated with RetroNectin as well as 1 additional well to serve as a mock/non-transduced control well for mock-transduced cells. Thus, 8 total wells were coated and prepared for transduction. Following coating, the plate was sealed and placed at 4°C overnight to allow for coating of wells.

The following day, day 0 of transduction, the RetroNectin-coated plate was allowed to acclimate to room temperature and RetroNectin solution was aspirated and replaced with complete culture medium consisting of RPMI 1640 medium (GE HyClone #SH30255.01) with 10% concentration of heat-inactivated fetal bovine serum (Corning #35-010-CV) and 1% concentration of penicillin/streptomycin solution (GE HyClone #SV30010). After addition of complete medium, the plate was placed in incubator for a brief incubation. During this time, titrated retroviral supernatants were thawed and brought to room temperature. Following

incubation, complete culture medium was aspirated and retroviral supernatant of respective h8F4-CAR codon-modified construct viral supernatant was added. For the mock/non-transduced control well, complete culture medium was added in lieu of retroviral supernatant. The plate was sealed and centrifuged at room temperature at 2000g for 90 minutes. During centrifugation, cultured Jurkat β cells for transduction were counted, pelleted, and resuspended in fresh complete culture medium at 150,000 cells per milliliter. Following centrifugation, retroviral supernatants were aspirated and discarded appropriately and replaced with Jurkat β cell suspension to 300,000 cells per transduction/well. The plate was re-sealed and centrifuged at 1000g for 30 minutes before placing in an incubator to begin culture.

At day 2 of transduction, half of existing medium in transduced cultures was removed and replaced with fresh complete medium. At day 3, the cells were removed from the RetroNectin-coated, non-tissue culture plate and counted. Cells were resuspended in complete medium and placed in 12-well tissue-culture-treated plates. Cells were counted every other day until day 7 and gradually scaled to larger culturing vessels such as 6-well tissue-culture-treated plates and T25 flasks. At day 7, cells were counted and an aliquot of culture was removed and prepared for transduction efficiency and analysis by flow cytometry.

Flow Cytometry Preparation and Staining

Following seven days after transducing h8F4-CAR unmodified and codon-modified constructs into Jurkat β cells, 2 million cells from each culture were removed and prepared for staining and analysis by flow cytometry. This included cells from each culture: unmodified-wildtype h8F4-CAR, S30, S7(i), S6(i), R27, R21(i), RS30(i), and control (mock-transduced) cultures.

Following removal from culture, cells were washed, centrifuged, and pelleted. Washed cells were resuspended using 250 μ L PBS to make 5 aliquots of 400,000 washed cells into independent FACS tubes to begin staining. Staining was split into five tubes per sample group including: a tube each for unstained sample, fluorescence-minus-one (FMO) stained sample, PR1/HLA-A2 tetramer (phycoerythrin (PE)-conjugated) stained sample, pp65/HLA-A2 tetramer stained sample (PE-conjugated) which served as an irrelevant control peptide stain, and Jackson ImmunoResearch goat anti-human IgG (H+L) F(ab')₂ fragment antibody (#109-006-088) stained sample (Alexa Fluor 647-conjugated) which binds to the hinge/stem region of h8F4-CAR. Each sample, except unstained samples, were also stained with Ghost Violet 510 viability dye (Tonbo #13-0870-T100) for live cell gating. Following incubation, cells were washed to remove excess antibody/tetramer, resuspended, fixed and stored until run on a BD LSR Fortessa cytometer.

Fluorescence-Activated Cell Sorting

Following day seven post-transduction flow cytometric analysis of surface expression and flow cytometry, cells were grown for another seven days and prepared for sorting into three populations using PR1/HLA-A2 tetramer. The three populations consisted of cells positive at a high avidity, positive at an intermediate avidity, and negative. 30 million cells were prepared for sorting from each sample group (S30, S7(i), S6(i), R27, R21(i), RS30(i), and unmodified) by washing, centrifuging, and pelleting cells. Cells were resuspended, strained, and stained with viability dye for live cell gating and PR1/HLA-A2 tetramer conjugated to phycoerythrin (PE) for sorting. After incubation, cells were washed twice to remove excess tetramer or viability dye and run through a cell strainer once more before resuspending cells. Cell sorting was performed by

the MD Anderson Advanced Cytometry & Sorting South Campus Core Facility. Sorting schemes are shown in Figure #7. After sorting, cells were centrifuged, pelleted, and resuspended in complete culture medium and maintained for two weeks to allow cells to recover viability and proliferate.

Day 7 Analysis of Transduced h8F4-CAR Cells Reveals Similar CAR Surface Expression

Analysis of samples run on cytometer revealed varying degrees of h8F4-CAR surface expression across all sample groups (S30, S7(i), S6(i), R27, R21(i), RS30(i), and unmodified). As expected, no surface expression of h8F4-CAR was detected in mock-transduced control cells. Surface expression was determined by percentage of positive binding of sample groups using PR1 tetramer as the direct antigen of h8F4-CAR and also anti-human IgG (H+L) F(ab')₂ fragment antibody which binds to the IgG1 CH2CH3 extracellular hinge/stem of h8F4-CAR. In addition, surface expression is further indicated by MFI (median fluorescence intensity) values of sample groups using these two staining agents. Percentage positive for binding as well as MFI values are shown in Figure #6. pp65/HLA-A2 tetramer was used as an irrelevant peptide control against h8F4-CAR and showed low levels of positive binding to h8F4-CAR constructs (data not shown). This can be explained as h8F4-CAR binds pp65/HLA-A2 peptide and tetramer in the context of HLA-A2 as part of its conformational epitope. pp65 peptide antigen is present as a result of cytomegalovirus (CMV) infection also in the context of HLA-A2 (35). PR1/HLA-A2 tetramer positive binding to h8F4-CAR constructs varied between 53.3-89.4% with less than 0.01% positive binding to mock-transduced cells. Anti-human IgG (H+L) antibody percentage positive binding to h8F4-CAR constructs varied between 52.3-89.3% with 0.16% positive binding to mock-

transduced cells. Surface expression variation across the h8F4-CAR constructs may be due to codon modification or as a result of transduction efficiency.

Figure #6. h8F4-CAR surface expression at day seven post-transduction using PR1 tetramer and anti-IgG (H+L) antibody that binds to h8F4-CAR stem.

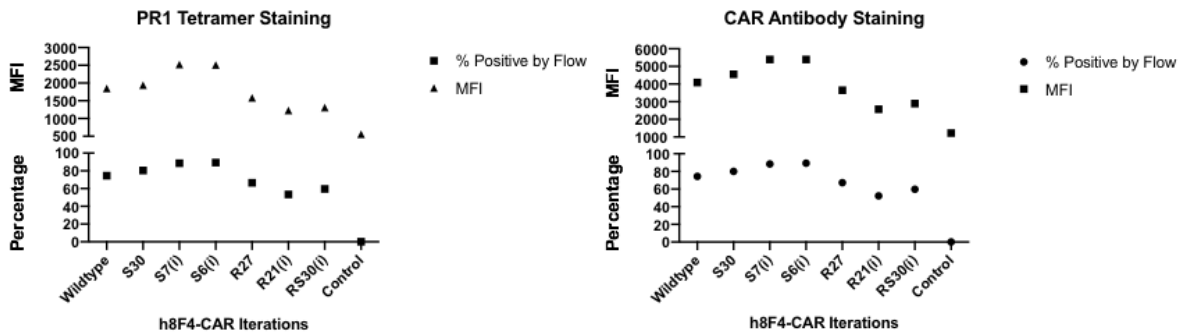


Figure #6. h8F4-CAR surface expression at day seven post-transduction. Surface expression visualized varies across the different h8F4-CAR constructs both unmodified and codon-modified. Values are shown as both percentage and median fluorescence intensity (MFI) values.

Flow Cytometric Surface Expression Patterns Remain Consistent and Indicates Effects of Rare Codon Modification

Sorting was conducted in order to further indicate the effects of rare codon modification by obtaining and studying purified populations. Once purified populations were obtained, deeper analysis could be conducted to test and study the effects of rare codon modification in h8F4-CAR compared to unsorted data obtained at the seven day post-transduction timepoint. This further analysis allows study of whether rare codon modification alters expression of h8F4-CAR as well

as potentially reveal effects of rare codon modification previously unseen at the seven day post-transduction timepoint. Additionally, sorting of these constructs into purified populations can further indicate rare codon modification effects on surface expression compared to unsorted populations which may be altered as a result of transduction efficiency.

Figure #7. Sorting scheme for PR1/HLA-A2 tetramer sorting of codon-modified constructs.

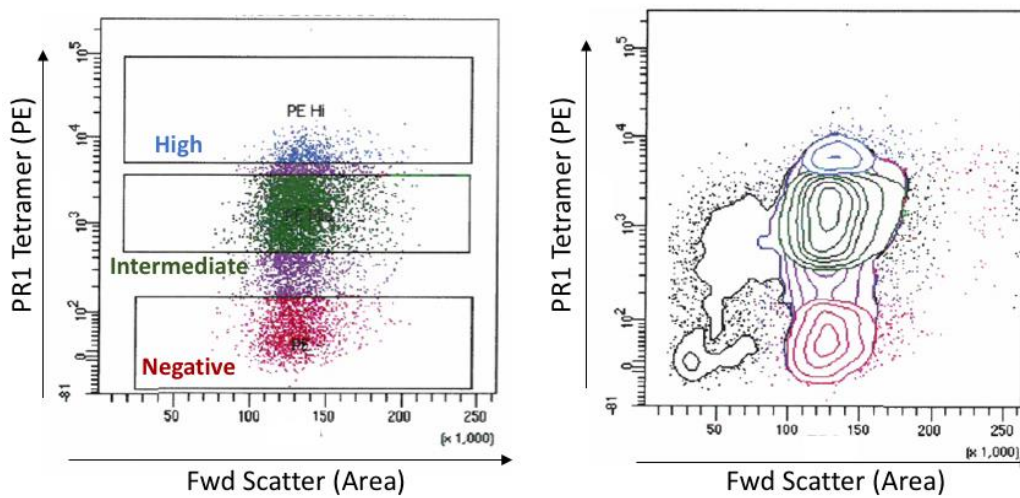


Figure #7. Sorting scheme for PR1/HLA-A2 tetramer sorting of codon-modified constructs. Sorting scheme and gating seen was maintained across sorting for all codon-modified constructs. High, intermediate, and negative populations were selected in order to study different avidities to PR1/HLA-A2 tetramer via additional assays.

Figure #8. Percentage positive binding and MFI values of sorted h8F4-CAR constructs at two weeks post-sort.

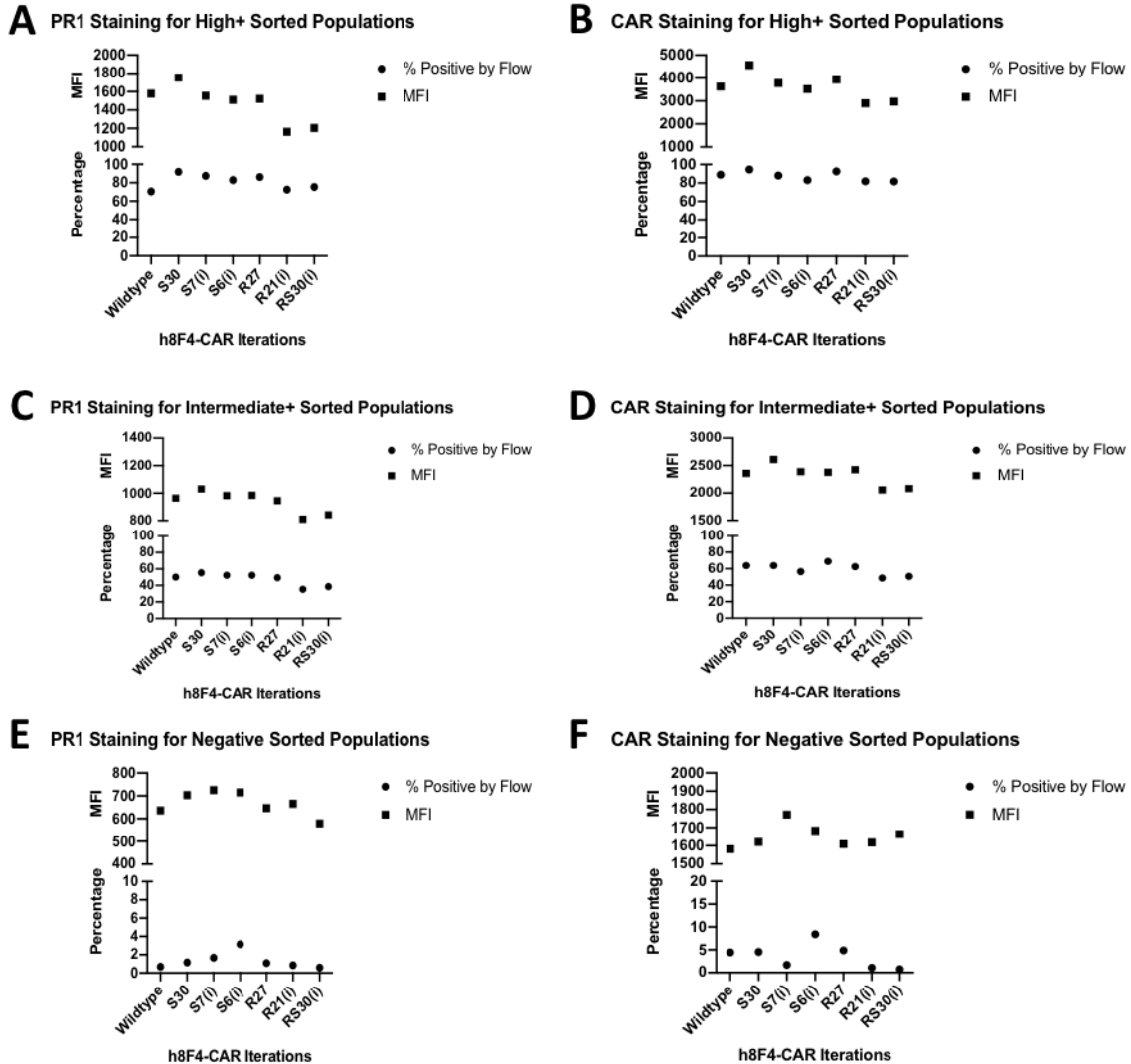


Figure #8. Percentage positive binding and MFI values of sorted h8F4-CAR constructs using PR1/HLA-A2 tetramer and human anti-IgG (H+L) which binds to the hinge/stem region of h8F4-CAR. PR1/HLA-A2 tetramer staining of high positive (A), intermediate positive (C), and negative (E) populations. Human anti-IgG (H+L) for h8F4-CAR hinge/stem binding stains of high positive (B), intermediate positive (C), and negative (F) populations. Cells were analyzed at these

timepoints to study whether h8F4-CAR cells persist and if expression changes over extended periods of time.

Day 7 post-transduction and two-week post-sorting timepoints were selected for two reasons. First, preliminary evaluation of h8F4-CAR surface expression at day 7 post-transduction would allow early identification of transduction success and efficiency. Second, analysis of cells two weeks post-sorting would allow assessment whether cells had continued expression of h8F4-CAR both persisted and was stable as well as verification of whether cells were indeed purified based on the sorting scheme.

Flow cytometry analysis of samples from two-week post-sorting timepoint revealed similar pattern of expression across sorted h8F4-CAR constructs that was seen in unsorted constructs. Percentage positive binding as well as MFI values are shown in Figure #8. This was notably indicated where the same constructs that exhibited a higher percentage positive and MFI value in the day seven post-transduction and unsorted flow cytometry analysis continued this same trend in the two week post-sort flow analysis. These trends revealed that surface expression did indeed vary across the different h8F4-CAR constructs. It is still possible that these variations occur as a result of transduction efficiency or codon modification. Since this timepoint studied cells that were sorted in purified populations, it is less likely that surface expression differences are a result of transduction efficiency and more indicative of the effects of rare codon modification. While retrovirus titration suggested theoretically that similar retrovirus physical titers would result in similar transduction efficiency, each experiment varies. Furthermore, different cell lines can also contribute to different infectious retroviral titers. Additionally, it is

possible and more likely that codon modification may be the cause of varying levels of surface expression. Deeper analysis of these constructs would certainly assist in elucidating this possibility. Therefore, additional experiments were performed such as immunoblotting.

Chapter 4: Immunoblotting of Codon-Modified h8F4-CAR Constructs

Protein Extraction from h8F4-CAR-Transduced Cells

Following flow cytometric analysis of codon-modified h8F4-CAR surface expression, differences of expression could also be studied using immunoblotting antibodies for h8F4-CAR. While flow cytometry can provide a first-look at surface expression following introduction of rare codon modification, immunoblotting can further elaborate and identify any potential effects that cannot be detected by flow cytometry by studying total protein and not what is only expressed at the cell surface. This included lysing of cells for protein isolation to conduct immunoblotting. Following transduction of h8F4-CAR codon-modified constructs into the mutant Jurkat cell line, Jurkat - β , cells were analyzed by flow cytometry for surface expression as seen in the previous chapter and in Figures #6 and 8. At the same timepoints cells were analyzed for surface expression by flow cytometry, cells were also lysed to conduct immunoblotting for h8F4-CAR. Immunoblotting was conducted to examine whether codon modification alters h8F4-CAR expression at the protein-level that could not be detected by flow cytometry.

Methodology

Cell Lysis & Protein Extraction

To lyse cells and isolate protein from transduced h8F4-CAR cells, cells were collected, washed thoroughly, and pelleted. Cells were resuspended in cell lysis buffer (consisting of 10mM/L HEPES (pH 7.9), 10mM/L KCl, 0.1mM/L EGTA, 0.1mM/L EDTA, 2mM/L DTT) supplemented with protease inhibitor (Thermo Scientific #78430) to prevent protease activity. Cells were thoroughly mixed and vortexed with lysis buffer, centrifuged to remove cell debris,

and supernatant (whole cell lysate) was collected and quantified. Whole cell lysate was quantified using the BioRad DC Protein Assay as instructed by manufacturer (BioRad #5000116). Quantified lysate was then used to conduct immunoblotting to probe for codon-modified h8F4-CAR. Cell lysates were used for immunoblotting assays for comparison with flow cytometry data. Both of these timepoints contained cells analyzed by flow cytometry from the same timepoints as seen in Figures #6 and 8.

Gel Electrophoresis and Immunoblotting

Following quantification, lysates were mixed with prepared denaturing loading buffer, briefly boiled, and loaded onto pre-cast protein gels (BioRad #456-1094) for electrophoresis using denaturing running buffer (BioRad #161-0772). Samples were electrophoresed and gel contents were transferred to PVDF membranes using the BioRad Trans-Blot Turbo RTA Transfer PVDF Kit and System as instructed by manufacturer (BioRad# 170-4272). Once transferred, membranes were blocked in blocking buffer (dry 5% non-fat milk in 1% TBS-Tween solution) for one hour before incubating in the following antibodies independently in blocking buffer overnight. Primary antibodies included:

- rabbit anti-human IgG antibody with predicted binding to h8F4-CAR IgG1 hinge/stem region (Abcam #ab109489) used at 1:250 dilution
- rabbit anti-human CD28 antibody with predicted binding to h8F4-CAR CD28 region (Cell Signaling #38774S) used at 1:500 dilution
- mouse anti-human CD3 ζ antibody with predicted binding to h8F4-CAR CD3 ζ region (Santa Cruz Biotechnology #sc-166435) used at 1:500 dilution

- mouse anti-human actin monoclonal antibody as a loading control (Millipore #MAB1501R) used at 1:2500 dilution
- goat anti-human IgG (H+L) AffiniPure F(ab')₂ fragment antibody with predicted binding to h8F4-CAR IgG1 hinge/stem region (Jackson ImmunoResearch #109-006-088) used at 1:250 dilution

Figure #9. Overview of relative predicted antibody recognition regions for primary immunoblotting antibodies used.

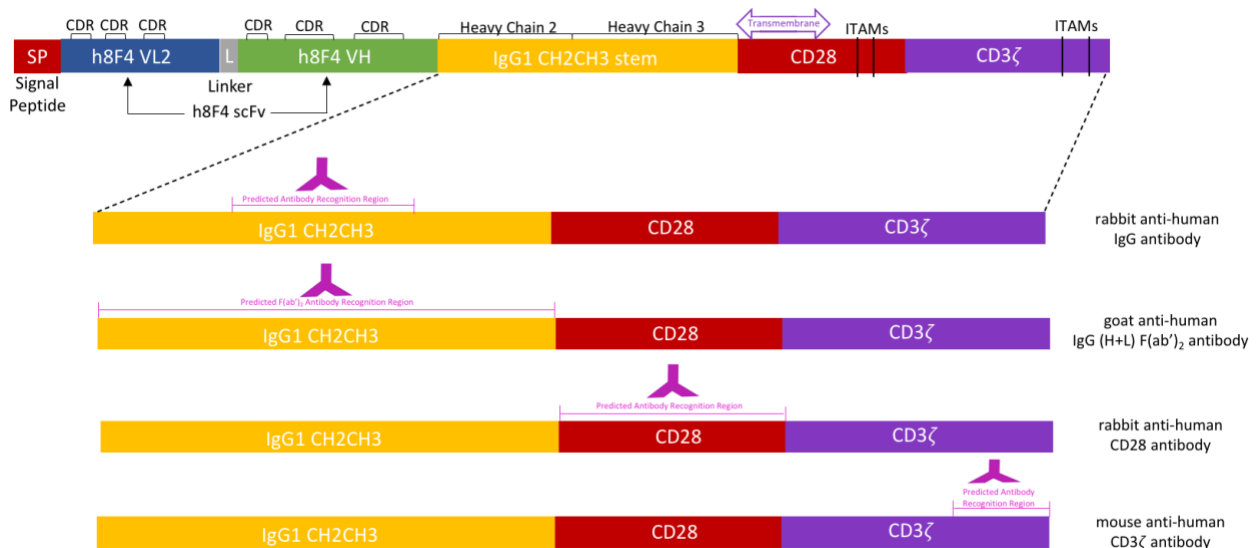


Figure #9. Predicted binding regions are shown in figure. Rabbit anti-human IgG antibody and mouse anti-human CD3ζ antibody have general predicted binding regions as specified by manufacturer. Goat anti-human IgG F(ab')₂ fragment antibody is a polyclonal antibody and rabbit anti-human CD28 antibody is a monoclonal antibody that binds endogenous total human CD28 as well as multiple CD28 isoforms.

Each primary antibody was independently incubated overnight with the exception of anti-actin primary antibody. Depending on host species of primary antibodies, secondary antibodies were used for detection of protein bands. Secondary antibodies included:

- goat anti-rabbit IgG HRP-linked antibody (Cell Signaling #7074S)
- horse anti-mouse IgG HRP-linked antibody (Cell Signaling #7076S)
- mouse anti-goat IgG HRP antibody (Santa Cruz Biotechnology #sc-2354)

All secondary antibodies were used at 1:1000 dilutions. Following overnight primary antibody incubation, membranes were washed thoroughly before incubating with secondary antibody in blocking buffer for one hour. Membranes were washed thoroughly again before developing using the Western Lightning Plus-ECL Kit (PerkinElmer #NEL103001EA) as instructed by manufacturer. Membranes were imaged using a BioRad ChemiDoc Touch Imaging System (Hercules, CA). Following each imaging of a membrane with a primary antibody (except actin) to detect h8F4-CAR, membranes were thoroughly washed and stripped of antibody using Restore Western Blot Stripping Buffer (Thermo Scientific #21059) according to manufacturer's instructions. Following membrane stripping, membranes were re-probed overnight with anti-actin primary antibody in blocking buffer, incubated in secondary antibody in blocking buffer for one hour, developed, and imaged with thorough washes in-between. Immunoblotting with anti-actin antibody after stripping membrane of previous primary antibody allowed verification of similar lysate loaded onto each gel as a loading control.

Lysates prepared at day 7 post-transduction were blotted following the steps previously mentioned with 50 μ g lysate per h8F4-CAR sample group (unmodified, S30, S7(i), S6(i), R27, R21(i), RS30(i), and mock-transduced/control). Each immunoblot was freshly done for each

primary antibody with the exception of anti-actin primary antibody which was done on same immunoblot after stripping to verify loading of sample as a control.

Immunoblotting Reveals Altered Expression of Codon-Modified h8F4-CAR

Day 7 post-transduction lysates were immunoblotted using each primary antibody in order to identify correct molecular weight bands for h8F4-CAR which has a molecular weight of 73kDa. Figure #10A shows immunoblotting for h8F4-CAR samples at day 7 post-transduction using primary rabbit anti-human IgG antibody which is predicted to bind to the IgG1 hinge/stem region of h8F4-CAR. Visualization of bands at correct molecular weight for h8F4-CAR confirm presence of h8F4-CAR as expected. However, interestingly, novel and unique bands in the S30 and R27 groups were visible at about 30kDa which were not present in unmodified, wildtype h8F4-CAR nor mock-transduced cells which serve as positive and negative controls, respectively. Presence of these novel bands in codon-modified constructs with rare codon modification spread extracellularly, transmembrane, and intracellularly indicate that codon modification may indeed result in a change in protein translation. Immunoblotting results for CD3 ζ are seen in Figure #10B and show the correct molecular weight for h8F4-CAR across all transduced samples at 73kDa as well as endogenous CD3 ζ which is naturally found in all T cells, including Jurkat - β cells. Endogenous CD3 ζ bands can be visualized across all samples as a dimer at 34kDa and as a monomer at 17kDa. It should be noted that the novel, unique bands seen in Figure #10A are not visualized in Figure #10B. The predicted binding epitope for the anti-CD3 ζ antibody lies at the C-terminal end of the h8F4-CAR-encoding sequence, therefore it may be a result of codon

modification causing pre-mature translational pausing and stop. This is discussed in greater detail in Chapter 5 of this thesis.

Figure #10. Immunoblotting of h8F4-CAR constructs at day 7 post-transduction.

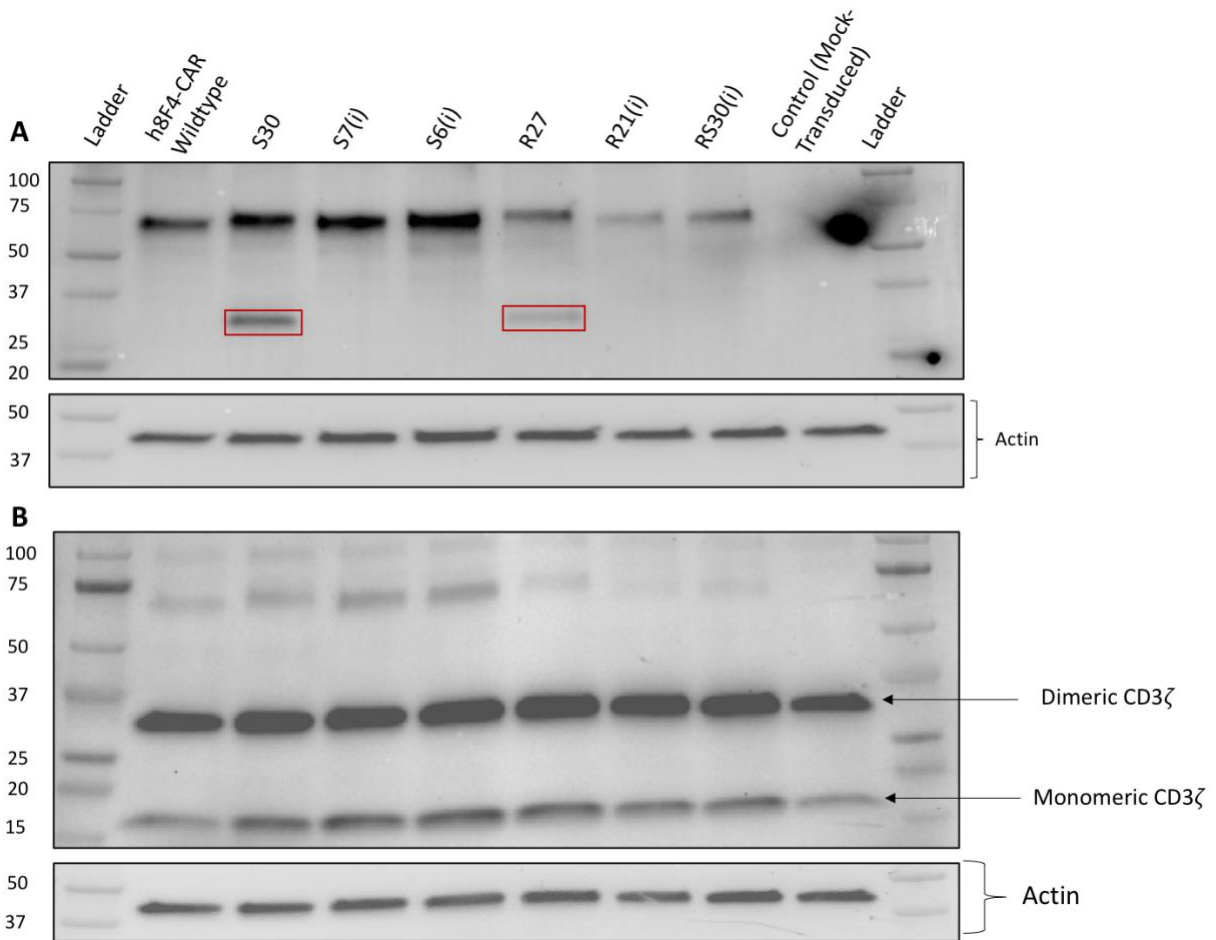


Figure #10. (A) Immunoblotting of sample groups at day 7 post-transduction using primary anti-human IgG antibody predicted to bind to IgG1 hinge/stem region of h8F4-CAR reveals expected bands signifying h8F4-CAR expression at 73kDa, but also reveals novel and unique bands (boxed in red) suspected to be a result of rare codon modification. **(B)** Immunoblotting of same groups at same timepoint using primary anti-human CD3 ζ antibody predicted to bind to CD3 ζ region of reveals expected bands but no novel/unique bands. Predicted binding region for this antibody

lies at the C-terminal end of sequence suggesting that some h8F4-CAR translational products result in pre-mature truncation.

Following sorting and flow cytometric analysis of sorted h8F4-CAR sample groups two weeks post-sorting (seen in Figures #7 and 8), these same cells from the same timepoint were also examined in greater detail via immunoblotting. Lysates prepared two weeks post-sorting were electrophoresed and blotted as previously described. Samples were split across three gels/membranes since sample groups consisted of unmodified, S30, S7(i), S6(i), R27, R21(i), and RS30(i) h8F4-CAR constructs that were sorted high positive, intermediate positive, and negative populations. Figure #11 shows membranes immunoblotted with rabbit anti-human IgG antibody revealing expected bands for h8F4-CAR at 73kDa as well as previously seen unique bands in constructs S30 and R27 at about 30kDa. A new set of novel bands is also visualized in constructs S30 and R27 at about 45kDa. Additionally, a novel band appears in the RS30(i) high positive sorted population at about 55kDa that was previously not detected. Immunoblotting using anti-human IgG (H+L) F(ab')₂ fragment antibody which is also predicted to bind to the h8F4-CAR IgG1 hinge/stem region reveals novel bands once again appear at the same molecular weights. This additional primary antibody probing h8F4-CAR across samples provides corroboratory evidence that indeed these novel and unique bands appear in codon-modified h8F4-CAR constructs as shown in Figure #12. These bands also appear most often in the S30 and R27 constructs with larger numbers of rare codon modification spanning the extracellular, transmembrane, and intracellular regions of the CAR sequence. Two unique bands also appear in the S7(i) high positive sorted populations at about 45kDa and another band at about 55-60kDa. While discussed in

greater detail in Chapter 5 of this thesis, previous studies investigating the role, usage and substitutions of codons within a sequence have yielded a variety of results and hypotheses suggesting that codon usage and selection have a variety of effects on translation of a sequence (32-35). Substitution of more commonly used codons in a sequence (optimization) has been shown to improve and maximize translation and expression. Substitution of rarer, less frequently used codons (modification) has been shown to cause translational inefficiencies. These inefficiencies are expected to be as a result of a myriad of mechanisms and effects such as ribosomal pausing, pre-mature truncation, and mRNA destabilization (37,38).

When blotted with anti-human CD28 and anti-human CD3 ζ predicted to bind to h8F4-CAR CD28 and CD3 ζ regions, no novel bands were detected as shown in Figures #13 and 14. Endogenous CD3 ζ can be seen as a dimer at 34kDa and as a monomer at 17kDa in Figure #13 and endogenous CD28 can be seen at about 39-40kDa in Figure #14. It is suspected that codon modification of h8F4-CAR results in defective translation with premature translational halting before translating regions where predicted binding epitopes are located. Additionally, endogenous CD28 and CD3 ζ bands at molecular weights similar to those seen using anti-IgG antibodies may mask unique band appearance. All novel bands appear selectively in these codon-modified h8F4-CAR iteration groups and were not seen in either unmodified, wildtype h8F4-CAR nor in negative sorted populations suggesting that these unique bands were likely a result of codon modification in h8F4-CAR.

Figure #11. Immunoblotting of h8F4-CAR constructs at two weeks post-sorting using anti-human IgG antibody.

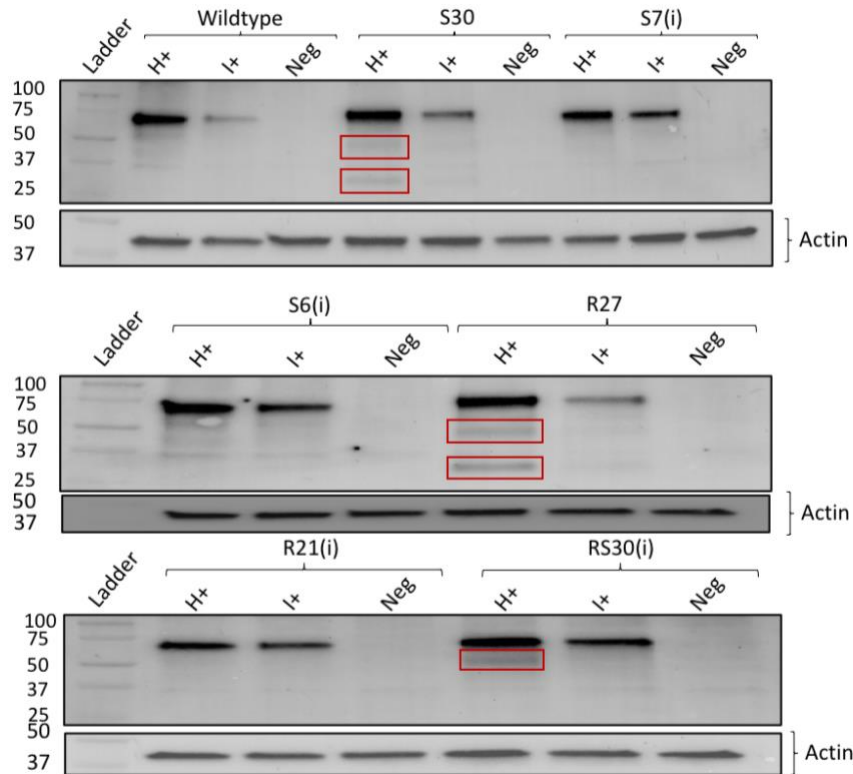


Figure #11. Immunoblot of sample groups at two weeks post-sorting using primary rabbit anti-human IgG antibody predicted to bind to IgG1 hinge/stem region of h8F4-CAR. Immunoblot reveals novel bands in codon-modified S30 and R27 constructs suggesting codon modification does alter h8F4-CAR expression. The appearance of these new and unique bands in the S30, R27, and RS30(i) constructs are in concordance with findings found in Hoekema et al (1987) where increasing numbers of rare codon substitutions in the PGK1 sequence in *S. cerevisiae* led to altered expressed of the cognate PGK1 protein. “H+” refers to cells sorted high positive, “I+” refers to cells sorted intermediate positive, and “Neg” refers to cells sorted as negative to PR1/HLA-A2 tetramer.

Figure #12. Corroboratory immunoblot evidence of codon modification effects altering h8F4-CAR expression.

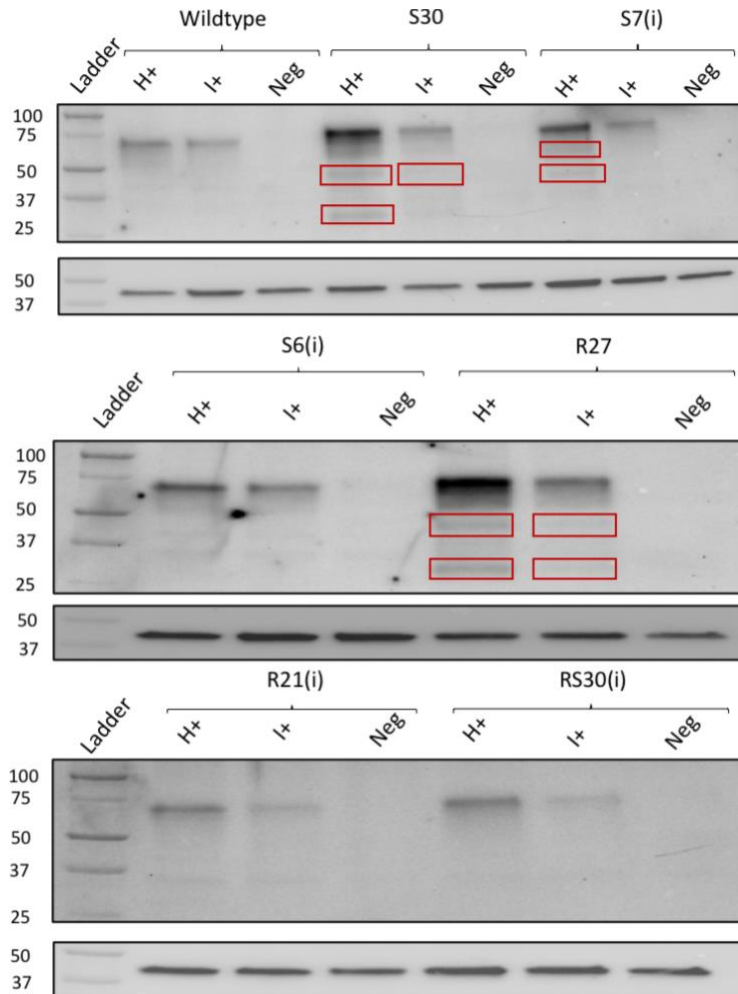


Figure #12. Immunoblot of sample groups at two weeks post-sorting using primary anti-human IgG (H+L) F(ab')₂ fragment antibody which is also predicted to bind to the h8F4-CAR IgG1 hinge/stem region. Data reveals corroboratory evidence of novel and unique bands in codon-modified constructs suggesting codon modification alters h8F4-CAR expression. Appearance of novel bands in the same constructs (S30 and R27) provide additional evidence of altered protein expression as a result of rare codon substitution. Appearance of novel and unique bands in the

S7(i) construct provide evidence that small numbers of codon modification intracellularly may also cause translational defectiveness but requires additional study.

Figure #13. CD3 ζ immunoblotting of h8F4-CAR constructs at two weeks post-sorting.

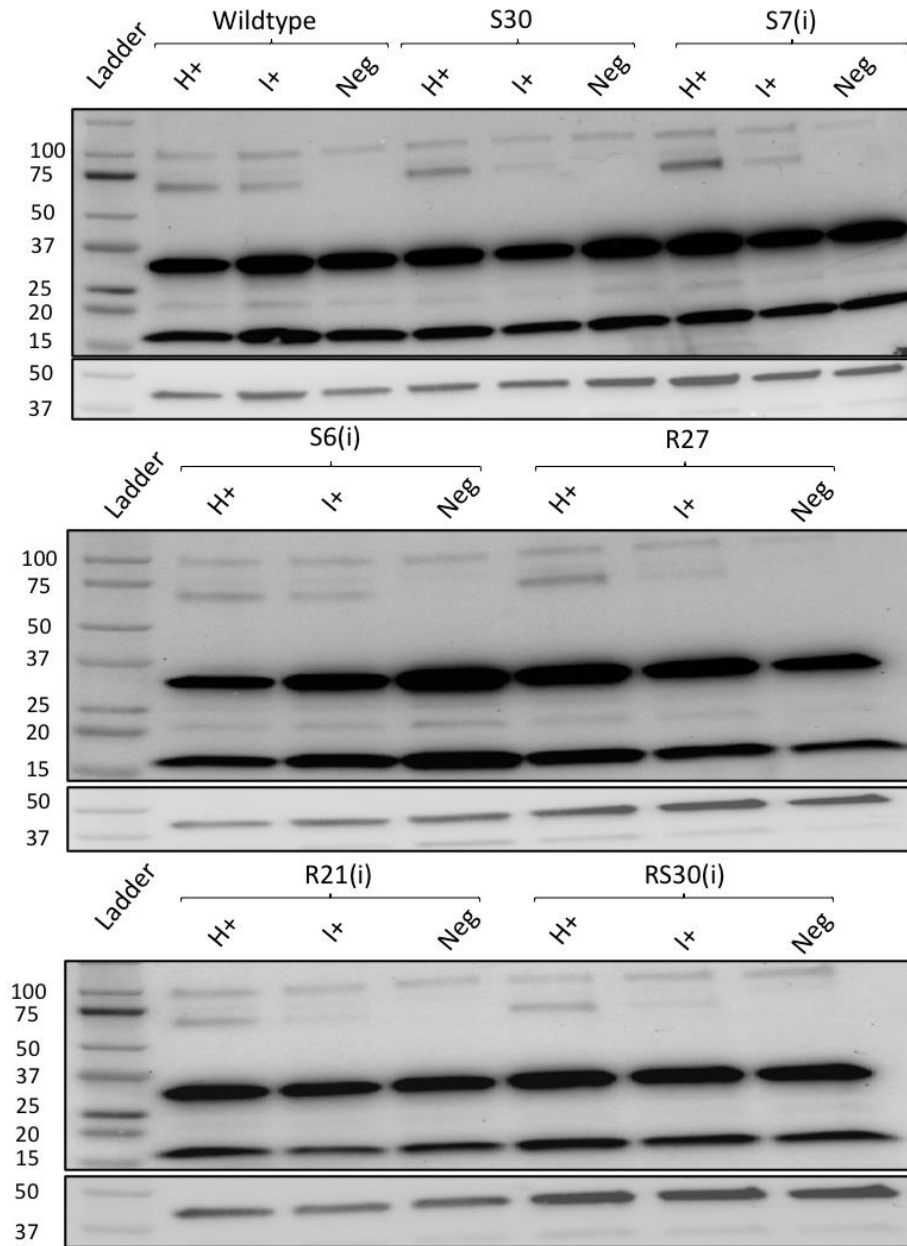


Figure #13. Immunoblot of sample groups at two weeks post-sorting using primary anti-human CD3 ζ antibody predicted to bind to CD3 ζ region of h8F4-CAR. Immunoblots do not reveal presence of novel bands seen in anti-IgG immunoblots suggesting that codon modification results in defective translation and pausing prior to reaching predicted binding sequence for this antibody.

Figure #14. CD28 immunoblotting of h8F4-CAR constructs at two weeks post-sorting.

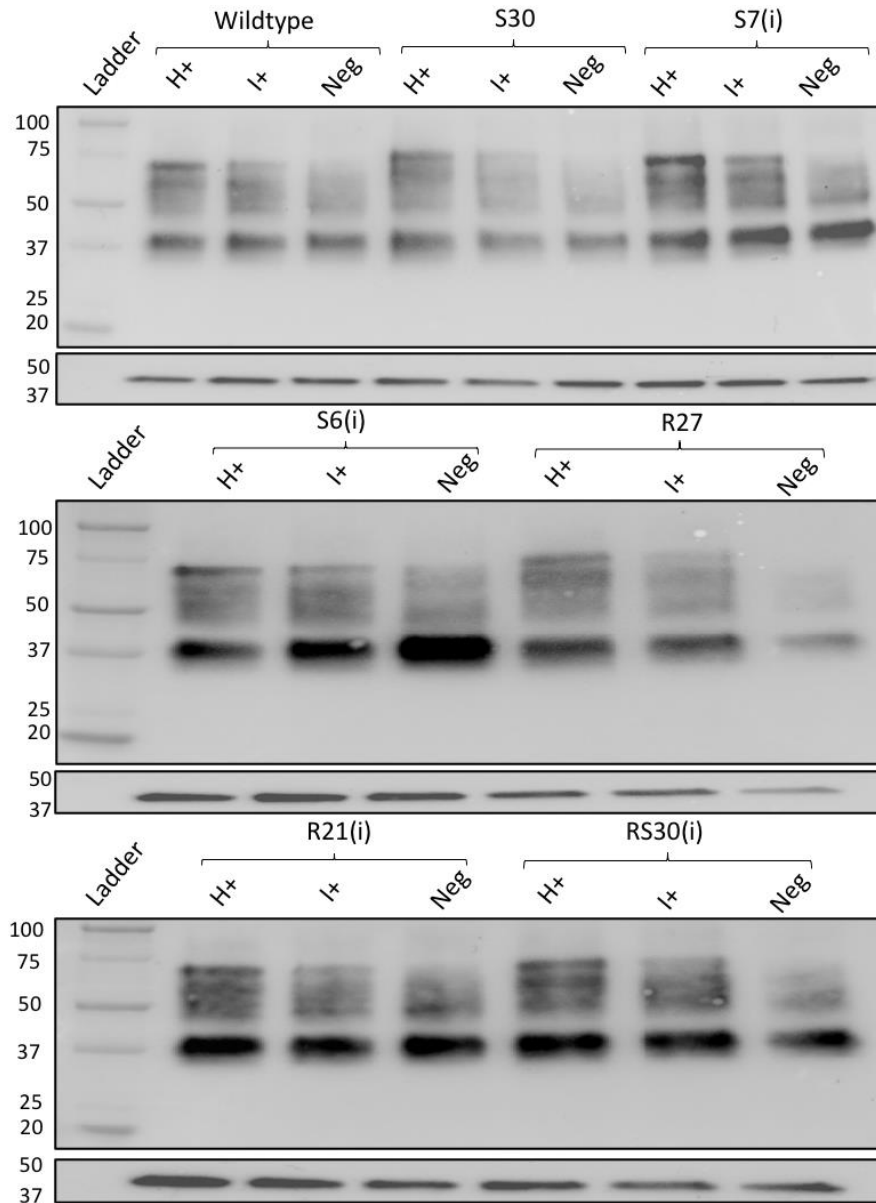


Figure #14. Immunoblotting of h8F4-CAR sorted populations using anti-CD28 antibody predicted to bind to CD28 region of h8F4-CAR. Blotting reveals correct bands for h8F4-CAR at 73kDa and shows endogenous CD28 across samples at 39-40kDa. Additional isoforms of CD28 are predicted to be bands between 40-70kDa as a result of alternative splicing according to manufacturer. It is again suspected that lack of novel/unique bands may be due to defective translation that halts

prior to reaching the antibody recognition portion of this antibody, or if there are indeed novel bands present, they are masked by endogenous CD28 and its isoforms.

Chapter 5: Discussion and Future Directions

Advances in the field of cancer immunotherapy for the treatment of a variety of cancers such as acute myeloid leukemia have been previously demonstrated (8,9). In particular, chimeric antigen receptor therapies against leukemias have shown success in pre-clinical studies treating AML and greater success in the clinic against B-ALL (22-27). This work presents foundational investigations into the improvement and optimization of a chimeric antigen receptor therapy for the treatment of PR1/HLA-A2+ malignancies. Furthermore, the implications of improving a therapy by the means presented in this work may hold utility and promise in the setting of CAR-T cell therapies as well as adoptive cellular therapies for a range of malignancies.

The ability to utilize genetic code degeneracy and codon bias has been demonstrated previously to develop and improve therapies for a variety of maladies (32-34). Two ways of utilizing the genetic code is codon optimization and codon modification. Codon optimization is the modification and substitution of codons within a sequence into their other codon counterparts that encode for the cognate amino acid at a higher frequency/fraction. Optimizing a sequence has been suggested to maximize and optimize output and expression of its cognate product (37). Codon modification is the modification and substitution of codons within a sequence into their other codon counterparts that encode for its cognate amino acid at a variety of frequencies to potentially tune output and expression of its product. The genetic code and its inherent codon bias holds potential to improve therapies that require tuning in order to optimize their function.

In the case of chimeric antigen receptor therapies, a common adverse effect of these therapies is unwanted on-target, off-tumor toxicity (28). This occurs when the target of a CAR-T

cell therapy is expressed both in normal and malignant cells and the therapy eliminates both instead of only malignant cells. When treating B-ALL using CD19 CAR-T cell therapy, on-target, off-tumor effects have been seen by targeting of CD19-expressing malignant cells and also healthy CD19-expressing cells resulting in B cell aplasia, or eradication (24,25,28). In cases like this, a solution is required. In this case, codon optimization in which protein/biologic expression is optimized and maximized, may be counterproductive and detrimental. However, utilizing rare codon modification to find unique modalities to tune and circumvent increased potential for on-target, off-tumor toxicity may provide a proactive technique to improve therapies. This work details the foundational studies applying the concept of codon modification into a chimeric antigen receptor therapy.

In this study, we investigated genetic code degeneracy and codon bias in a 2nd generation chimeric antigen receptor named h8F4-CAR which targets PR1/HLA-A2-expressing blasts (17). This was investigated by strategically introducing rare codons into the sequence to determine whether this would alter CAR expression, retain specificity, and identify a manner in which avidity/affinity of the CAR could be modulated. A codon usage frequency table for the human genome was used to investigate, identify, and study rare codons present with the human genome. Once these were determined, they were studied within h8F4-CAR for location, density, and frequency. The rare codons TCG and CGT for serine and arginine, respectively, were selected and endogenous codons within specified regions of h8F4-CAR were modified and substituted into these rare codons. Because there are a variety of permutations in which codon modification could be applied to h8F4-CAR, six constructs were developed to study some of these permutations such as location (extracellular, transmembrane, or intracellular), density (more

dense in a given location), or amino acid (15+ amino acids each with their own rare codon(s)). The six constructs are shown schematically in Figure #3.

Results from a four-week time course study following transduction of the six constructs as well as unmodified, “wildtype” h8F4-CAR post-transduction in the mutant Jurkat cell line (Jurkat - β) show that surface expression varies between constructs but is stable and persists. Varied surface expression may be attributed to two possible factors. The first is that transduction efficiency varied between the constructs. However, physical viral titration of the viral supernatants used to transduce the cells revealed similar titers which suggest similar transduction efficiency. Additionally sorting into pure populations makes the rationale for transduction efficiency causing the difference in surface expression less likely. The second, and most likely, is that codon modification may be a cause of varied surface expression. While expression was varied, percentage positive for either PR1/HLA-A2 tetramer or anti-IgG antibody which binds to the h8F4-CAR hinge/stem as well as MFI values show that the variation is subtle between groups. Groups were loosely classified into serine-modified constructs (S7(i), S6(i), and S30) and arginine-modified constructs (R21(i), RS30(i), and R27). The RS30(i) construct was grouped with the arginine-modified constructs since the majority of codons modified were arginine (21 codons) compared to serine (9 codons). In the serine-modified constructs, MFI for each construct was similar or higher compared to wildtype, unmodified h8F4-CAR. In the arginine-modified constructs, MFI for each construct was similar or reduced compared to the wildtype. Consistency in results between both timepoints by flow cytometry supports that rare codon modification alters surface expression. However, additional methods to detect differences

in h8F4-CAR expression such as immunoblotting were conducted and indeed revealed more pronounced effects of rare codon modification on expression.

Additionally, to conduct deeper analysis of codon-modified constructs, sorting was conducted to purify transduced cultures using PR1/HLA-A2 tetramer. Cells were sorted into high positive, intermediate positive, and negative populations. Once sorted, each population would be able to be further analyzed to identify any possible effects of codon modification and rare codon substitution in h8F4-CAR that could not be detected by flow cytometry. In addition to sorting a negative population of cells to have negative sample to draw result comparisons from, presence of non-surface expressed h8F4-CAR could be detected when conducting immunoblotting or any future assays. Presence of non-surface expressed h8F4-CAR in surface-stained FACS negative populations could be attributed to inefficient or defective translation that would not transport to the cell surface or prevent surface detection due to a defective product.

The principle of codon optimization and modification takes basis from a variety of observations, evidences, and hypotheses that seek to explain inherent codon bias within the genetic code. Evidence of the effects of altering codons in models and systems are not lacking. Ward et al. demonstrated the promise of codon optimization in a potential gene therapy to treat human factor VIII deficiency which is a cause of hemophilia A (32). Hoekema et al. demonstrated the effects of introducing increasing numbers of rare codons via substitution and modification in the PGK1 gene in *Saccharomyces cerevisiae* which led to decreased expression of the PGK1 protein (35). Scholten et al. demonstrated improvement in expression of transgenic T cell receptors when codon optimizing α and β chains (33). Schutsky et al. demonstrated modest but notable improvement in a transient CAR therapy platform when sequences were codon

optimized (34). Altogether, codon optimization and modification do indeed alter expression; however, the mechanism by which this occurs has not been definitively determined. It is possible that codon bias is a result of evolution to prefer codons that allow the most efficient translation of products. Similarly, the effects of codon bias in genetic sequences and altering the codons within them can result in defective/inefficient translation, ribosomal pausing, truncation of product, protein misfolding, mRNA destabilization, and mRNA degradation (38).

While results seen from flow cytometry analysis of codon-modified h8F4-CAR constructs do not directly show the effects of codon modification and substitution, immunoblotting of these groups, both unsorted and sorted, clearly indicate alteration of h8F4-CAR. Figures #10A, 11, and 12 reveal novel and unique bands when probed using human anti-IgG antibodies to detect h8F4-CAR. Each immunoblot reveals the expected bands at the correct molecular weight for h8F4-CAR; however, novel and unique bands appear in the S30 and R27 constructs with some exceptions for the S7(i) and RS30(i) constructs which also contain novel bands. It is possible that these bands were isoforms of h8F4-CAR that have appeared as a result of codon modification and rare codon substitution. These bands were clearly not seen in unmodified, wildtype h8F4-CAR nor mock-transduced cells or negative sorted populations. It is possible that rare codon introduction may have caused premature truncation, ribosomal pausing, or defective translation. Figures #10B, 13, and 14 do not show presence of any novel or unique bands which may be due to two factors. First, translational issues caused by codon modification may result in premature truncation, defective translation, or ribosomal pausing prior to reaching the predicted binding region for the anti-CD28 and/or anti-CD3 ζ antibodies. This would not allow detection of novel/unique bands. Second, endogenous CD28 and CD3 ζ bands that were present in Jurkat - β cells may mask any

bands that appear as a result of codon modification. Overall, codon modification does indeed seem to cause alterations to h8F4-CAR that are more evident by immunoblotting.

Future directions for this study include studying the functionality of each of these codon-modified constructs via cytotoxicity and signaling assays in both HLA-A2+ and HLA-A2- human peripheral blood mononuclear cells. Assessment of cytotoxic capabilities of each construct has the potential to elucidate whether changes made at the codon and nucleic acid level have larger downstream implications through transcription, translation, and eventually surface expression and functionality. Since costimulatory and signaling domains of h8F4-CAR were codon-modified, it is also imperative to assess whether any differences in signaling capabilities have resulted compared to unmodified h8F4-CAR. Additionally, it is important to assess whether codon modification results in any transcriptional or amplification differences since codons were changed. This can be studied by designing primer/probe sets for the constructs and assay by reverse transcriptase quantitative polymerase chain reaction (RT-qPCR) experiments.

To continue studying novel bands in codon-modified constructs, mass spectrometry can be employed to identify the contents of each band. This would not only allow determination of what the contents of the bands are but also allow identification whether the final amino acid within the sequence is a serine or arginine residue. If the final residue in the sequence is a serine or arginine residue, this would indicate that translation was halted at a codon-modified residue further providing evidence that codon modification indeed altered h8F4-CAR expression. Furthermore, it is important to also study whether these effects could be reversed or modulated. This could be possible through further study of tRNA pools for the cognate rare codons and possible exogenous tRNA therapy to try and reverse alternate product production. Altogether,

further studies, particularly functional studies, would elucidate and clarify the potential of using the genetic code and inherent codon bias to reveal a unique modality to tune CAR-T cell therapies and adoptive cellular therapies as a whole using the methods described in this work.

Figure #15. Future directions for h8F4-CAR codon modifications.

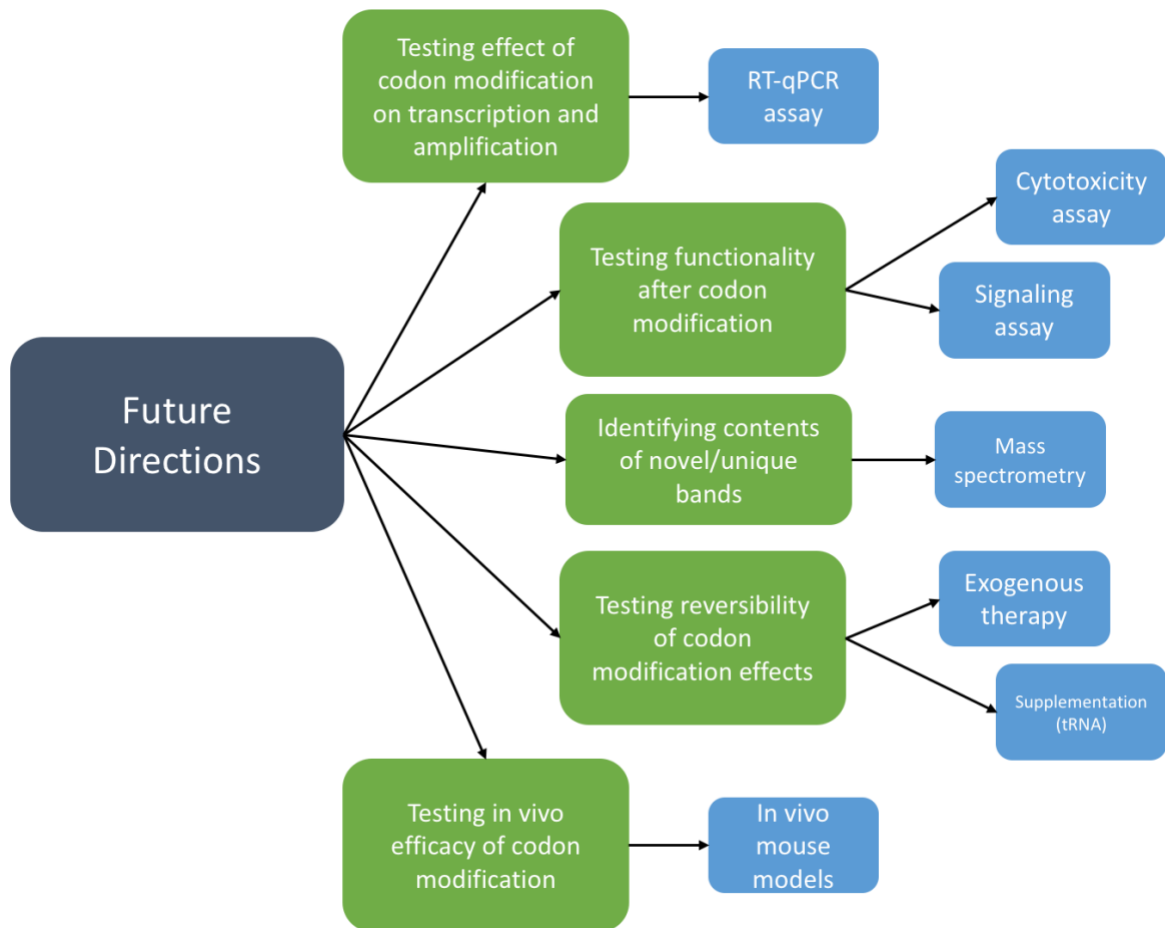


Figure #15. These experiments seek to continue studying the implications of using the natural genetic code to beneficially improve and enhance biologic therapies such as h8F4-CAR as well as other CAR and adoptive cell therapies. Additional experiments are critical to continue studying the effect of codon modification to build on the findings and promise of this work.

The aims of this project sought to develop and construct sequences encoding h8F4-CAR with the introduction of rare codon modifications in order to test and determine the ability to reveal an innovative method to modulate h8F4-CAR expression to avoid increased potential for on-target, off-tumor toxicity. By strategically constructing and developing these h8F4-CAR constructs bearing various permutations of rare codon modification, this created the foundational groundwork to study the potential of rare codon modification in CAR therapies. Additionally, testing and determining the effects of introducing rare codon modification allowed a first-look at the effects on expression. As supported by flow cytometry and immunoblotting data, the introduction of rare codons into h8F4-CAR indeed alters expression in the majority of the rare codon-modified constructs. This is also supported by the subtle changes in surface expression across the codon-modified constructs compared to wildtype, unmodified h8F4-CAR, and is further supported to a greater extent by the appearance of novel and unique bands in codon-modified constructs (S30, S7(i), RS30(i), and R27) by immunoblotting. Together, this supports our hypothesis that introduction of rare synonymous codon modifications to h8F4-CAR reduce and alter its expression as seen in 4 of the 6 rare codon-modified constructs. This further lays the groundwork for studying the genetic code, codon bias, and rare codon modification as a unique and innovative method to improve CAR therapies that target self-antigens and reduce the potential for on-target, off-tumor toxicity.

In summary, the data presented in this work demonstrates the foundation upon which therapies can harness the genetic code and codon bias to find unique methods to improve therapies using its own genetic sequence. We demonstrate that 1) construction of rare codon-modified h8F4-CAR is possible; 2) codon-modified constructs can still express h8F4-CAR at the

cell surface and at proper molecular weight; 3) h8F4-CAR is indeed altered in certain codon-modified constructs; and 4) this is evidenced by appearance of novel and unique bands seen in immunoblots. We set steps forward to continue testing codon modification as a method to improve and modulate h8F4-CAR therapy by 1) preparing to test and assay transcriptional and transcriptional amplification differences by RT-qPCR; 2) conduct deeper analysis of novel and unique bands found in immunoblots by mass spectrometry; 3) assess the functionality of each codon-modified h8F4-CAR construct by conducting in vitro assays such as cytotoxicity and signaling assays; and 4) investigate methods to reverse possible translational issues caused by rare codon modification such as exogenous cognate tRNA therapy or supplementation for the rare codons. Together these steps seek to continue validating results and pursue utilizing the genetic code as a unique method to improve and enhance CAR and adoptive cellular therapies. The data presented merits further investigation and study into codon modification of h8F4-CAR as well as the mechanism of how codon modification alters h8F4-CAR expression and where this alteration occurs.

Bibliography

1. Khwaja, A., Bjorkholm, M., Gale, R.E., Levinem R.L., Jordan, C.T., Ehninger, G., Bloomfield, C.D., Estey, E., Burnett, A., Cornelissen, J.J., Scheinberg, D.A., Bouscary, D., and Linch, D.C. 2016. Acute myeloid leukaemia. *Nature Reviews Disease Primers* 2.
2. Dohner, H., Weisdorf, D.J., Bloomfield, C.D. Acute myeloid leukemia. *The New England Journal of Medicine* 373: 1136-52.
3. Acute Myeloid Leukemia - Cancer Stat Facts. 2020. SEER. <https://seer.cancer.gov/statfacts/html/amyl.html>. Accessed April 20, 2020.
4. The Cancer Genome Atlas Research Network. 2013. Genomic and epigenomic landscapes of adult de novo acute myeloid leukemia. *The New England Journal of Medicine* 368(22): 2059-74.
5. Perl, A.E., Altman, J.K., Cortes, J., Smith, C., Litzow, M., Baer, M.R., Claxton, D., Erba, H.P., Gill, S., Goldberg, S., Jurcic, J.G., Larson, R.A., Liu, C., Ritchie, E., Schiller, G., Spira, A.I., Strickland, S.A., Tibes, R., Ustun, C., Wang, E.S., Stuart, R., Rollig, C., Neubauer, A., Martinelli, G., Bahceci, E., and Levis, M. 2017. Selective inhibition of FLT3 by gilteritinib in relapsed/refractory acute myeloid leukemia: A multicenter, first-in-human, open-label, phase 1/2 study. *Lancet Oncology* 18(8): 1061-75.
6. Murphy, K., Travers, P., Walport, M., and Janeway, C. 2012. *Janeway's Immunobiology*. Garland Science, New York, NY.
7. Shang, Y., and Zhou, F. 2019. Current advances in immunotherapy for acute leukemia: An overview of antibody, chimeric antigen receptor, immune checkpoint, and natural killer. *Frontiers in Oncology* 9(917).

8. Jen, E.Y., Ko, C.W., Lee, J.E., Del Valle, P.L., Aydanian, A., Jewell, C., Norsworthy, K.J., Przepiorka, D., Nie, L., Liu, J., Sheth, C.M., Shapiro, M., Farrell, A.T., and Pazdur, R. 2018. FDA approval: Gemtuzumab ozogamicin for the treatment of adults with newly diagnosed CD33-positive acute myeloid leukemia. *Clinical Cancer Research* 24(14): 3242-6.
9. Pizzitola, I., Anjos-Afonso, F., Rouault-Pierre, F., Lassailly, F., Tettamanti, S., Spinelli, O., Biondi, A., Biagi, E., and Bonnet, D. 2014. Chimeric antigen receptors against CD33/CD123 antigens efficiently target primary acute myeloid leukemia cells in vivo. *Leukemia* 28: 1596-1605.
10. Horowitz, M.M, Gale, R.P., Sondel, P.M., Goldman, J.M., Kersey, J., Kolb, H.J., Rimm, A.A., Ringden, O. Rozman, C., Speck, B., Truitt, R.L., Zwaan, F.E., and Bortin, M.M. 1990. Graft-versus-leukemia reactions after bone marrow transplantation. *Blood* 75(3): 555-62.
11. Kolb, H.J. 2008. Graft-versus-leukemia effects of transplantation and donor lymphocytes. *Blood* 112(12): 4371-83.
12. Anguille, S., Van Tendeloo, V.F., and Bememan, Z.N. 2012. Leukemia-associated antigens and their relevance to the immunotherapy of acute myeloid leukemia. *Leukemia* 26: 2186-96.
13. Cheever, M.A., Allison, J.P., Ferris, A.S., Finn, O.J., Hastings, B.M., Hecht, T.T., Mellman, I., Prindiville, S.A., Steinman, R.M., Viner, J.L., Weiner, L.M., and Matrisian, L.M. 2009. The prioritization of cancer antigens: A National Cancer Institute pilot project for the acceleration of translational research. *Clinical Cancer Research* 15(17): 5323-37.
14. Molldrem, J.J., Dermime, S., Parker, K., Jiang, Y.Z., Mavroudis, D., Hensel, N., Fukushima, P., and Barrett, A.J. 1996. Targeted T-cell therapy for human leukemia: Cytotoxic T

- lymphocytes specific for a peptide derived from proteinase 3 preferentially lyse human myeloid leukemia cells. *Blood* 88(7): 2450-7.
15. Molldrem, J.J., Clave, E., Jiang, Y.Z., Mavroudis, D., Raptis, A., Hensel, N., Agarwala, V., and Barrett, A.J. 1997. Cytotoxic T lymphocytes specific for a nonpolymorphic proteinase 3 peptide preferentially inhibit chronic myeloid leukemia colony-forming units. *Blood* 90(7): 2529-34.
16. Molldrem, J.J., Lee, P.P., Wang, C., Felio, K., Kantarjian, H.M., Champlin, R.E., and Davis, M.M. 2000. Evidence that specific T lymphocytes may participate in the elimination of chronic myelogenous leukemia. *Nature Medicine* 6: 1018-23.
17. Ma, Q., Wang, C., Jones, D., Quintanilla, K.E., Li, D., Wang, Y., Wieder, E.C., Clise-Dwyer, K., Alatrash, G., You, M.J., Lu, S., Qazilbash, M.H., and Molldrem, J.J. 2010. Adoptive transfer of PR1 cytotoxic T lymphocytes associated with reduced leukemia burden in a mouse acute myeloid leukemia xenograft model. *Cytotherapy* 12(8): 1056-62.
18. Qazilbash, M.H., Wieder, E., Thall, P.F., Wang, X., Rios, R., Lu, S., Kanodia, S., Ruisaard, K.E., Giralt, S.A., Estey, E.H., Cortes, J., Komanduri, K.V., Clise-Dwyer, K., Alatrash, G., Ma, Q., Champlin, R.E., and Molldrem, J.J. 2017. PR1 peptide vaccine induces specific immunity with clinical responses in myeloid malignancies. *Leukemia* 31(3): 697-704.
19. Sergeeva, A., Alatrash, G., He, H., Ruisaard, K.E., Lu, S., Wygant, J., McIntyre, B.W., Ma, Q., Li, D., St John, L., Clise-Dwyer, K., and Molldrem, J.J. 2011. An anti-PR1/HLA-A2 T-cell receptor-like antibody mediates complement-dependent cytotoxicity against acute myeloid leukemia progenitor cells. *Blood* 117(16): 4262-72.

20. Sergeeva, A., He, H., Ruisaard, K.E., St John, L., Alatrash, G., Clise-Dwyer, K., Li, D., Patenia, R., Hong, R., Sukhumalchandra, P., You, M.J., Gagea, M., Ma, Q., and Molldrem, J.J. 2016. Activity of 8F4, a T cell receptor-like anti-PR1/HLA-A2 antibody, against primary human AML in vivo. *Leukemia* 30(7): 1475-84.
21. Herrmann, A.C., Im, J.S., Pareek, S., Ruiz-Vasquez, W., Lu, S., Sergeeva, A., Mehrens, J., He, H., Alatrash, G., Sukhumalchandra, P., St John, L., Clise-Dwyer, K., Zha, D., and Molldrem, J.J. 2019. A novel T-cell engaging bi-specific antibody targeting the leukemia antigen PR1/HLA-A2. *Frontiers in Immunology* 9 (3153).
22. Ma, Q., Garber, H.R., Lu, S., He, H., Tallis, E., Ding, X., Sergeeva, A., Wood, M.S., Dotti, G., Salvado, B., Ruissard, K., Clise-Dwyer, K., St John, L., Rezvani, K., Alatrash, G., Shpall, E.J., and Molldrem, J.J. 2016. A novel TCR-like CAR with specificity for PR1/HLA-A2 effectively targets myeloid leukemia in vitro when expressed in human adult peripheral blood and cord blood T cells expressed in human adult peripheral blood and cord blood T cells. *Cytotherapy* 18(8): 985-94.
23. Jackson, H.J., Rafiq, S., and Brentjens, R.J. 2016. Driving CAR T-cells forward. *Nature Reviews Clinical Oncology* 13: 370-83.
24. Maude, S.L., Frey, N., Shaw, P.A., Aplenc, R., Barrett, D.M., Bunin, N.J., Chew, A., Gonzalez, V.E., Zheng, Z., Lacey, S.F., Mahnke, Y.D., Melenhorst, J.J., Rheingold, S.R., Shen, A., Teachey, D.T., Levine, B.L., June, C.H., Porter, D.L., and Grupp, S.A. 2014. Chimeric antigen receptor T cells for sustained remissions in leukemia. *The New England Journal of Medicine* 371(16): 1507-17.

25. Brentjens, R.J., Davila, M.L., Riviere, I., Park, J., Wang, X., Cowell, L.G., Bartido, S., Stefanski, J., Taylor, C., Olszweska, M., Borquez-Ojeda, O., Qu, J., Wasielewska, T., He, Q., Bernal, Y., Rijo, I.V., Hedvat, C., Kobos, R., Curran, K., Steinherz, P., Jurcic, J., Rosenblat, T., Maslak, P., and Sadelain, M. 2013. CD19-targeted T cells rapidly induce molecular remissions in adults with chemotherapy-refractory acute lymphoblastic leukemia. *Science Translational Medicine* 5(177).
26. Sadelain, M. 2017. CD19 CAR T cells. *Cell* 171.
27. Kenderian, S.S., Ruella, M., Shestova, O., Klichinsky, M., Aikawa, V., Morrissette, J.J.D., Scholler, J., Song, D., Porter, D.L., Carroll, M., June, C.H., and Gill, S. 2015. CD33-specific chimeric antigen receptor T cells exhibit potent preclinical activity against human acute myeloid leukemia. *Leukemia* 29: 1637-47.
28. Brudno, J.N. and Kochenderfer, J.N. 2016. Toxicities of chimeric antigen receptor T cells: Recognition and management. *Blood* 127(26): 3321-30.
29. Cheng, J., Zhao, L., Zhang, Y., Qin, Y., Guan, Y., Zhang, T., Liu, C., and Zhou, J. 2019. Understanding the mechanisms of resistance to CAR T-cell therapy in malignancies. *Frontiers in Oncology* 9: 1237.
30. Gargett, T. and Brown, M.P. 2014. The inducible caspase-9 suicide gene system as a “safety switch” to limit on-target, off-tumor toxicities of chimeric antigen receptor T cells. *Frontiers in Pharmacology* 5(235).
31. Beatty, G.L., Haas, A.R., Maus, M.V., Torigian, D.A., Soulen, M.C., Plesa, G., Chew, A., Zhao, Y., Levine, B.L., Albelda, S.M., Kalos, M., June, C.H. 2014. Mesothelin-specific chimeric

- antigen receptor mRNA-engineered T cells induce anti-tumor activity in solid malignancies. *Cancer Immunol Res* 2(2): 112-20.
32. Ward, N.J., Buckley, S.M.K., Waddington, S.N., VandenDriessche, T., Chuah, M.K.L., Nathwani, A.C., McIntosh, J., Tuddenham, E.G.D., Kinnon, C., Thrasher, A.J., and McVey J.H. 2011. Codon optimization of human factor VIII cDNAs leads to high-level expression. *Blood* 117(3): 798-807.
33. Scholten, K.B.J., Kramer, D., Kueter, E.W.M., Graf, M., Schoedl, T., Meijer, C.J.L.M., Schreuers, M.W.J., and Hooijberg, E. 2006. Codon modification of T cell receptors allows enhanced functional expression in transgenic human T cells. *Clinical Immunology* 119: 135-45.
34. Schutsky, K., Song, D.G., Lynn, R., Smith, J.B., Poussin, M., Figini, M., Zhao, Y., and Powell, D.J. 2015. Rigorous optimization and validation of potent RNA CAR T cell therapy for the treatment of common epithelial cancers expressing folate receptor. *Oncotarget* 6(30): 28911-28.
35. Hoekema, A., Kastelein, R.A., Vasser, M., and de Boer, H.A. 1987. Codon replacement in the PGK1 gene of *Saccharomyces cerevisiae*: Experimental approach to study the role of biased codon usage in gene expression. *Molecular and Cellular Biology* 7(8): 2914-24.
36. Solache, A., Morgan, C.L., Dodi, A.I., Morte, C., Scott, I., Baboonian, C., Zal, B., Goldman, J., Grundy, J.E., and Madrigal, J.A. 1999. Identification of three HLA-A*0201-restricted cytotoxic T cell epitopes in the cytomegalovirus protein pp65 that are conserved between eight strains of the virus. *Journal of Immunology* 163: 5512-18.

37. Gustafsson, C., Govindarajan, S., and Minshull, J. 2004. Codon bias and heterologous protein expression. *Trends in Biotechnology* 22(7): 347-53.
38. Hanson, G. and Collier, J. 2018. Codon optimality, bias and usage in translation and mRNA decay. *Nat Rev Mol Cell Biol* 19(1): 20-30.

Vita

Rolando Antonio Vedia was born in Laredo, Texas, the son of Roxanna Isela Vedia and Jose Antonio Vedia. After completing his work at United High School, Laredo, Texas in 2013, he entered Texas A&M International University in Laredo, Texas. He received the degree of Bachelor of Science with a major in biology from Texas A&M International University in December 2016, graduating cum laude. For the next seven months, he worked as a laboratory assistant in the Department of Biology & Chemistry at Texas A&M International University in Laredo, Texas. In August of 2017 he entered The University of Texas MD Anderson Cancer Center UTHealth Graduate School of Biomedical Sciences.

Permanent address:

2400 McCullough Ave #12088,
San Antonio, Texas 78212